1997

Delta(1232) and the polarizabilities of the nucleon

TR Hemmert

BR Holstein
holstein@physics.umass.edu

J Kambor

$\Delta(1232)$ and the Polarizabilities of the Nucleon*

Thomas R. Hemmert[a], Barry R. Holstein,[b] and Joachim Kambor[c]

[a] Theory Division, TRIUMF, 4004 Wesbrook Mall
Vancouver, BC V6T 2A3, CANADA

[b] Department of Physics and Astronomy, University of Massachusetts
Amherst, MA 01003, USA

[c] Theoretische Physik, Universität Zürich
CH-8057 Zürich, Switzerland

February 1, 2008

ZU-TH-34/96
TRI-PP-96-68

Abstract

Previous calculations of the polarizabilities of the nucleon within the framework of heavy baryon chiral perturbation theory have included the contribution of the $\Delta(1232)$ only in its effects on various contact terms or have been performed in chiral SU(3) where systematic errors are difficult to control. Herein we perform a corresponding calculation in chiral SU(2) wherein $\Delta(1232)$ is treated as an explicit degree of freedom and the expansion is taken to third order in soft momenta, the pion mass and the quantity $M_\Delta - M_N$, collectively denoted ϵ. We present the results of a systematic $\mathcal{O}(\epsilon^3)$ calculation of forward Compton scattering off the nucleon, extract the electric polarizability $\bar{\alpha}_E$, the magnetic polarizability $\bar{\beta}_M$ and the spin polarizability γ and compare with available information from experiments and from previous calculations. Concluding with a critical discussion of our results, we point out the necessity of a future $\mathcal{O}(\epsilon^4)$ calculation.

* Research supported in part by the National Science and Engineering Research Council of Canada, by the U.S. National Science Foundation and by Schweizerischer Nationalfonds.

1 Introduction

Understanding of the implications of QCD within the regime of low energy physics has during the past decade become accessible via the technique of chiral perturbation theory (ChPT) [1]. Initial applications were in the arena of Goldstone boson interactions [2] together with a few calculations in the baryon sector [3, 4], using relativistic baryon ChPT. In recent years use of so-called heavy baryon methods [5, 6] has generated much interest in calculations involving baryons and a great deal of work has been done studying strong, weak, and electro-magnetic physics in the near threshold region [7]. In this work we will focus on SU(2) heavy baryon chiral perturbation theory (HBChPT), which has become the most fully developed sector within baryon ChPT [7, 8, 9]. Thus-far, consistent extension to higher energies in SU(2) HBChPT has been limited by treatment of the important $\Delta(1232)$ resonance only in terms of its contribution to the various counterterms which arise in such calculations. The technique by which to address this deficiency was developed some time ago [10] by including the $\Delta(1232)$ as an explicit degree of freedom in a chiral perturbative scheme[1]. Recently, a reformulation of this formalism which allows for a systematic and explicit calculation of higher order terms in an expansion of soft momenta, the pion mass and the mass difference $m_\Delta - m_N$ has been given,[12, 13] and in this note we apply this technique to the problem of forward nucleon Compton scattering and the polarizabilities of the nucleon. Nucleon Compton scattering is an area of research which has recently received a great deal of attention, both experimentally and theoretically and in the next section we review the status of such work. In section 3 we give a brief introduction to the formalism necessary to include the $\Delta(1232)$ in chiral calculations, and in section 4 apply this to evaluate delta contributions to $N - \gamma$ scattering, examine its influence on the polarizabilities and give a critical discussion of our $\mathcal{O}(\epsilon^3)$ results. Finally, in a concluding section 5 we summarize our findings.

[1]Using the formalism of [10], Butler and Savage [11] have given an estimate of the contribution of the spin 3/2 resonances to the electric and magnetic polarizabilities of the nucleon. However, this calculation was performed in SU(3) and made a number of approximations, so that a direct comparison with systematic SU(2) work is not possible.

2 Compton Review

To lowest order the spin-averaged amplitude for Compton scattering on the nucleon is given by the Thomson amplitude

$$\text{Amp} = -\frac{Q^2}{M}\hat{\epsilon}\cdot\hat{\epsilon}' \tag{1}$$

where Q, M represent the nucleon charge, mass and $\hat{\epsilon}, \hat{\epsilon}'$ and $k_\mu = (\omega, \vec{k}), k'_\mu = (\omega', \vec{k}')$ specify the polarization vectors and four-momenta of the initial,final photons respectively. In next order are generated contributions arising from electric and magnetic polarizabilities—$\bar{\alpha}_E$ and $\bar{\beta}_M$—which measure the response of the nucleon to the application of quasi-static electric and magnetic fields

$$\text{Amp} = \hat{\epsilon}\cdot\hat{\epsilon}'\left(-\frac{Q^2}{M} + \omega\omega'\, 4\pi\bar{\alpha}_E\right) + \hat{\epsilon}\times\vec{k}\cdot\hat{\epsilon}'\times\vec{k}'\, 4\pi\bar{\beta}_M + \mathcal{O}(\omega^4)\,. \tag{2}$$

The associated differential scattering cross section on the proton is given by

$$\begin{aligned}\frac{d\sigma}{d\Omega} &= \left(\frac{e^2}{4\pi M}\right)^2\left(\frac{\omega'}{\omega}\right)^2\Big[\frac{1}{2}(1+\cos^2\theta) \\ &- \frac{4\pi M\omega\omega'}{e^2}\left(\frac{1}{2}(\bar{\alpha}_E+\bar{\beta}_M)(1+\cos\theta)^2 + \frac{1}{2}(\bar{\alpha}_E-\bar{\beta}_M)(1-\cos\theta)^2\right) + \ldots\Big]\end{aligned} \tag{3}$$

Thus by measurement of the differential Compton scattering cross section one can extract the electric and magnetic polarizabilities, provided

i) the energy is large enough that these terms are significant with respect to the Thomson contribution but

ii) not so large that higher order effects dominate.

This has been accomplished for the proton in the energy regime 50 MeV$<$ ω $<$100 MeV, yielding[14]

$$\bar{\alpha}_E^p = (11.6\pm0.6\pm0.6)\times10^{-4}\text{fm}^3; \qquad \bar{\beta}_M^p = (2.6\mp0.6\mp0.6)\times10^{-4}\text{fm}^3 \tag{4}$$

(Note: In practice one generally uses the results of unitarity and the validity of the forward scattering dispersion relation which yields the Baldin sum rule

$$\bar{\alpha}_E^p + \bar{\beta}_M^p = \frac{1}{2\pi^2}\int_0^\infty \frac{d\omega}{\omega^2}\sigma_{\rm tot}^p(\omega) = (14.2 \pm 0.3) \times 10^{-4}{\rm fm}^3 \qquad (5)$$

as a constraint, since the uncertainty associated with the integral over the photo-absorption cross section $\sigma_{\rm tot}(\omega)$ is smaller than that associated with the polarizability measurements.)

Since the neutron has no charge, such a Thomson-polarizability interference experiment is not possible, so alternative methods must be used. The most precise measurement involves a recent n-Pb scattering experiment, wherein the dipole moment induced in the moving neutron due to the nuclear charge acts back on the Pb nucleus. This second order process and the resulting $1/r^4$ interaction proportional to the electric polarizability can be detected in a transmission experiment via the characteristic linear dependence on the beam momentum k. This experiment was recently performed at ORNL and yielded results[15]

$$\bar{\alpha}_E^n = (12.6 \pm 1.5 \pm 2.0) \times 10^{-4}{\rm fm}^3; \qquad \bar{\beta}_M^n = (3.2 \mp 1.5 \mp 2.0) \times 10^{-4}{\rm fm}^3 \quad (6)$$

quite similar to those of the proton. (In this experiment only the electric polarizability is measured directly. However, using the unitarity sum rule result

$$\bar{\alpha}_E^n + \bar{\beta}_M^n = \frac{1}{2\pi^2}\int_0^\infty \frac{d\omega}{\omega^2}\sigma_{\rm tot}^n(\omega) = (15.8 \pm 0.5) \times 10^{-4}{\rm fm}^3 \qquad (7)$$

the magnetic polarizability can be extracted.)

On the theoretical side, constituent quark-based approaches which rely on the sum rule[16]

$$\bar{\alpha}_E = \frac{1}{3M} < \sum_{i=1}^{3} e_i(\vec{r}_i - \vec{R}_{cm})^2 > +2\sum_{n\neq 0}\frac{|<n|\sum_{i=1}^3 e_i(\vec{r}_i - \vec{R}_{cm})_z|0>|^2}{E_n - E_0} \quad (8)$$

are bound to fail since the sum over intermediate states component of Eq.(8) is in almost any reasonable model identical for both neutron or proton, leading to a prediction

$$\bar{\alpha}_E^p - \bar{\alpha}_E^n \simeq \frac{\alpha}{3M}(< r_p^2 > - < r_n^2 >) = 4.2 \times 10^{-4}{\rm fm}^3 \qquad (9)$$

in conflict with the experimental result that $\bar{\alpha}_E^n > \bar{\alpha}_E^p$.[18] The solution to the problem lies in a proper treatment of the pion degrees of freedom of the nucleon, which is suggested by the feature that the leading pion loop contributions to neutron and proton are identical, in agreement with experiment. The problem can best be addressed using the technique of heavy baryon chiral perturbation theory [7], within which at $\mathcal{O}(p^3)$ one finds a result [8]

$$\bar{\alpha}_E^p = \bar{\alpha}_E^n = 10\bar{\beta}_M^p = 10\bar{\beta}_M^n = \frac{5\alpha g_A^2}{96\pi F_\pi^2 m_\pi} = 12.2 \times 10^{-4}\text{fm}^3 \qquad (10)$$

This $\mathcal{O}(p^3)$ calculation represents the leading result for $\bar{\alpha}_E$ and $\bar{\beta}_M$ in ChPT, but gets the qualitative features of the polarizabilities right and even agreement with experiment ! The results diverge as $1/m_\pi$ in the chiral limit, giving support to the idea that at these low energies the photon interacts primarily with the long-range pion cloud of the nucleon. In order to understand the experimental finding that $\bar{\alpha}_E^n > \bar{\alpha}_E^p$ the leading ChPT result is not sufficient. One must include higher order terms in order to find isospin dependent effects and to judge the convergence behaviour of the series[2] . A calculation at $\mathcal{O}(p^4)$ has been performed by Bernard, Kaiser, Schmidt and Meißner [20]. At this order four counterterms are required, which were estimated by BKSM by treating higher resonances—including the delta resonance—as very heavy with respect to the nucleon. The results of this process are

$$\begin{aligned} \bar{\alpha}_E^p &= (10.5 \pm 2.0) \times 10^{-4}\text{fm}^3; \quad \bar{\beta}_M^p = (3.5 \pm 3.6) \times 10^{-4}\text{fm}^3 \\ \bar{\alpha}_E^n &= (13.4 \pm 1.5) \times 10^{-4}\text{fm}^3; \quad \bar{\beta}_M^n = (7.8 \pm 3.6) \times 10^{-4}\text{fm}^3 \end{aligned} \qquad (11)$$

where the uncertainty is associated with the counterterm contribution from the Δ and from K, η loop effects. A very interesting aspect of this $\mathcal{O}(p^4)$ calculation lies in the fact that it identifies a mechanism to counter the large positive contribution on $\bar{\beta}_M$ due to $\Delta(1232)$ resonance exchange, which is a well-known problem in calculations of the magnetic polarizability via effective lagrangians [17]. BKSM found that at $\mathcal{O}(p^4)$ (negative) $N\pi$-loop contributions can essentially balance out the (positive) Delta effects hidden in the counterterms ! Nevertheless, we observe that the uncertainties of their $\mathcal{O}(p^4)$ calculation are quite dramatic so that real understanding of the ChPT

[2]Higher order corrections to the $\mathcal{O}(p^3)$ HBChPT results for the polarizabilities have been discussed by L'vov [19].

predictions for the polarizabilities will require more work. In particular, the large uncertainty in $\bar{\beta}_M$ is mainly related to poorly known couplings involving $\Delta(1232)$, which was used to determine some of the counterterms via "resonance saturation". If one retains $\Delta(1232)$ as an explicit degree of freedom in the chiral calculation, as done in our $\mathcal{O}(\epsilon^3)$ calculation of section 4, one can in principle determine all delta couplings of interest from (other) experiments in a systematic fashion. Furthermore, one does not limit oneself to the narrow scope of "resonance saturation" for the spin 3/2 contributions. We refer to section 4 for further discussion of this point.

Finally, with respect to the magnetic polarizability, we note that the simple quark model *can* provide a basic understanding of experiment. The prediction[16]

$$\begin{aligned} \bar{\beta}_M &= -\frac{1}{2M}(\sum_i e_i(\vec{r}_i - \vec{R}_{cm})^2 > -\frac{1}{6} < \sum_i e_i^2(\vec{r}_i - \vec{R}_{cm})^2/m_i > \\ &+ 2\sum_{n\neq 0} \frac{| < n| \sum_i \frac{e_i}{2m_i}\sigma_{iz}|0 > |^2}{E_n - E_0} \end{aligned} \tag{12}$$

involves a substantial diamagnetic recoil contribution

$$\bar{\beta}_M^{\rm dia} = \left\{ \begin{array}{ll} -10.2 \times 10^{-4}{\rm fm}^3 & p \\ -8.5 \times 10^{-4}{\rm fm}^3 & n \end{array} \right. \tag{13}$$

which when added to the large paramagnetic contribution due to the $\Delta(1232)$[21]

$$\bar{\beta}_M^{\Delta} = \left\{ \begin{array}{ll} +12 \times 10^{-4}{\rm fm}^3 & p \\ +12 \times 10^{-4}{\rm fm}^3 & n \end{array} \right. \tag{14}$$

gives results in basic agreement with the experimental findings. Hence, it is clear that proper inclusion of the Δ degrees of freedom is essential.

When spin-dependence is included the situation becomes somewhat more complex. In order to simplify the present exploratory analysis, we restrict our attention to forward scattering, in which case the amplitude can be written as

$$\mathrm{Amp} = f_1(\omega)\ \hat{\epsilon}\cdot\hat{\epsilon}' + i\vec{\sigma}\cdot(\hat{\epsilon}'\times\hat{\epsilon})\ \omega\ f_2(\omega) \tag{15}$$

where $f_1(\omega), f_2(\omega)$ are both even functions under crossing—$\omega \to -\omega$—and are therefore functions only of ω^2. In terms of our previous notation we have

$$f_1(\omega) = -\frac{e^2}{4\pi M} + (\bar{\alpha}_E + \bar{\beta}_M)\omega^2 + \ldots \tag{16}$$

while in the case of $f_2(\omega)$ we can make a similar expansion[22]

$$f_2(\omega) = -\frac{e^2\kappa^2}{2M^2} + \gamma\omega^2 + \ldots \tag{17}$$

where κ is the anomalous magnetic moment of the target and the new structure γ is the "spin-polarizability." As in the case of $f_1(\omega)$ the form of the leading term in the expansion is dictated by rigorous low energy theorems, while the ω^2 correction represents a probe of hadronic structure. One difference between the spin-dependent and spin-averaged amplitudes, however, is the asymptotic behavior as $\omega \to \infty$. The better behavior of $f_2(\omega)$ suggested by Regge theory allows one to write an unsubtracted dispersion relation in this case, leading to the strictures[23]

$$\begin{aligned} \frac{\pi e^2\kappa^2}{2M^2} &= -\int_0^\infty \frac{d\omega}{\omega}[\sigma_-(\omega) - \sigma_+(\omega)] \\ \gamma &= \frac{1}{4\pi^2}\int_0^\infty \frac{d\omega}{\omega^3}[\sigma_-(\omega) - \sigma_+(\omega)] \end{aligned} \tag{18}$$

where $\sigma_\pm(\omega)$ are the photo-absorption cross sections for parallel and anti-parallel alignments of photon and target helicities. The first of these relations—the Drell-Hearn-Gerasimov (DHG) sum rule—has received a good deal of attention recently. On the experimental side, efforts are being mounted to measure the spin-dependent structure function $f_2(\omega)$ directly, thereby confirming the prediction of the low energy theorem.[24] However, this has not yet been achieved. On the theoretical end, there have been a number of attempts to evaluate the dispersive integral of the DHG using what information currently exists for the photo-absorption cross sections. The existing data set is incomplete in that helicity-dependent cross sections have not yet been measured. Thus one uses existing multipole decompositions from *unpolarized* experiments in order to perform the analysis. Such decompositions are available, however, only in the single pion production channel so that above the two pion threshold model-dependent assumptions

must be made. With this caveat present results are somewhat higher than predicted by the low energy theorem

$$\begin{aligned} \frac{\pi e^2 \kappa_p^2}{2M^2} &= 0.167\text{GeV}^{-2} \\ -\int_0^\infty \frac{d\omega}{\omega}[\sigma_-(\omega)-\sigma_+(\omega)]^{\text{multipole}} &= \begin{cases} 0.208\text{GeV}^{-2} & \text{Karliner[25]} \\ 0.210\text{GeV}^{-2} & \text{Workman/Arndt[26]} \\ 0.182\text{GeV}^{-2} & \text{Burkert/Li[27]} \end{cases} \end{aligned} \tag{19}$$

and there have even been arguments made that challenge the assumptions under which the DHG form was derived.[28] However, resolution of these problems awaits reliable helicity-dependent cross section measurements, which should be available in the near future.[3]

Using the same multipole analysis it is possible to evaluate the dispersion integral involving the spin dependent polarizability, yielding[29]

$$\gamma = \frac{1}{4\pi^2}\int_0^\infty \frac{d\omega}{\omega^3}[\sigma_-(\omega)-\sigma_+(\omega)]^{\text{multipole}} = \begin{cases} -1.3\times 10^{-4}\text{fm}^{-4} & p \\ -0.4\times 10^{-4}\text{fm}^{-4} & n \end{cases} \tag{20}$$

For a detailed discussion of the contributions of the various nucleon resonances to the sum rules of Eq.(18) and the problems of the constituent quark model in describing the DHG sum rule we refer the reader to the review article by Drechsel [30].

These results are in dramatic disagreement with the $\mathcal{O}(p^3)$ ChPT predictions[8]

$$\gamma_p = \gamma_n = \frac{e^2 g_A^2}{96\pi^3 F_\pi^2 m_\pi^2} = +\,4.4\times 10^{-4}\text{fm}^{-4} \tag{21}$$

Unlike the case of $\bar{\alpha}_E$ and $\bar{\beta}_M$, at present there exists no corresponding $\mathcal{O}(p^4)$ ChPT calculation that reconciles this discrepancy. Presently the best information about the sub-leading behaviour of γ comes from a relativistic baryon ChPT calculation at the one-loop level [8], yielding

$$\gamma_p^{1-\text{loop}} = +2.2\times 10^{-4}\text{ fm}^4 \quad \gamma_n^{1-\text{loop}} = +3.2\times 10^{-4}\text{ fm}^4\,. \tag{22}$$

[3] A second area of interest is in the generalization of the DHG form to include the deep inelastic region and its connection with the integrated spin dependent structure function $g_1(k^2)$. However, we shall not discuss this issue herein.

This calculation does not resolve the discrepancy with the multipole analysis results of Eq.(20). However, it is known from phenomenological considerations[4] that $\Delta(1232)$ makes a major contribution of opposite sign. In section 4.2 we present a systematic chiral calculation of γ with nucleons, deltas and pions as explicit degrees of freedom.

Having given a brief summary of current research in this area we now proceed to outline the formalism which allows inclusion of the $\Delta(1232)$ in a consistent chiral power counting framework.

3 Small Scale Expansion in HBChPT

The subject of SU(2) Heavy Baryon ChPT of nucleons and pions has been well developed in recent years [8, 7]. In the conventional form one organizes the calculation according to an $\mathcal{O}(p^n)$ powercounting, where p denotes either a soft momentum or the pion mass m_π. All nucleon resonances, strange particles, vector mesons, etc. are integrated out, i.e. they only appear in higher order contact interactions. For near threshold processes this program has proved highly successful–for an outstanding review of the field we refer the reader to ref. [7]. However, phenomenologically it is known that in the nucleon sector the first nucleon resonance–$\Delta(1232)$–lies very close to the nucleon and can exert its influence even to processes at very low energies. This special situation in the baryon sector has early on [10] prompted suggestions to keep the spin-3/2 baryon resonances as explicit degrees of freedom in the chiral lagrangian in order to include all relevant physics and to improve the convergence of the perturbation series.

If one retains $\Delta(1232)$ as an explicit degree of freedom in SU(2) HBChPT, one is faced with an additional dimensionful parameter $\Delta = M_\Delta - M_N$, which corresponds to the mass splitting between the nucleon and the delta resonance in the chiral limit. Phenomenologically Δ is a small parameter of ≈ 300 MeV which, unlike m_π remains finite in the chiral limit. As was shown in refs. [10, 12, 13] one can nevertheless set up a consistent field-theoretic HBChPT formalism provided one organizes the calculation according to an $\mathcal{O}(\epsilon^n)$ powercounting, where ϵ now denotes a small scale of either a soft momentum, the pion mass or the mass splitting Δ. Our formalism has been constructed in such a way, that an $\mathcal{O}(\epsilon^n)$ result *automatically* contains any

[4]This has also been pointed out by the authors of [8].

$\mathcal{O}(p^n)$ result in [7] plus additional terms involving the $\Delta(1232)$ resonance which might be present to the order we are calculating.

In our calculation of Compton scattering below, which is done to $\mathcal{O}(\epsilon^3)$ in the small scale expansion, we shall need only the lowest order vertices, the propagator involving the $\Delta(1232)$, as well as possible counterterm contributions to $NN\gamma$, $NN\gamma\gamma$, and $N\Delta\gamma$. Details of how this can be achieved in a general $1/M$ expansion are given in ref. [12, 13]. Here we list only the minimal results necessary for the present calculation.

The systematic 1/M-expansion of the coupled $N\Delta$-system starts with the most general chiral invariant lagrangian involving relativistic spin 1/2 (ψ_N) and spin 3/2 (ψ_μ) fields [5]

$$\mathcal{L} = \mathcal{L}_N + \mathcal{L}_\Delta + (\mathcal{L}_{\Delta N} + h.c.) \tag{23}$$

with

$$\begin{aligned}
\mathcal{L}_\Delta &= \bar{\psi}_i^\mu \, \Lambda_{\mu\nu}^{ij} \, \psi_j^\nu \\
\Lambda_{\mu\nu}^{ij} &= -\Big[(i \not{D}^{ij} - M_\Delta \, \delta^{ij}) g_{\mu\nu} - \frac{1}{4}\gamma_\mu\gamma^\lambda(i \not{D}^{ij} - M_\Delta \, \delta^{ij})\gamma_\lambda\gamma_\nu \\
&\quad + \frac{g_1}{2} g_{\mu\nu} \not{u}^{ij}\gamma_5 + \frac{g_2}{2}(\gamma_\mu u_\nu^{ij} + u_\mu^{ij}\gamma_\nu)\gamma_5 + \frac{g_3}{2}\gamma_\mu \not{u}^{ij}\gamma_5\gamma_\nu\Big] + ... \\
\mathcal{L}_N &= \bar{\psi}_N \left(i \not{D} - M_N + \frac{g_A}{2} \not{u}\gamma_5 \right) \psi_N + ... \\
\mathcal{L}_{\Delta N} &= g_{\pi N\Delta} \, \bar{\psi}_i^\mu \, (g_{\mu\nu} + z\gamma_\mu\gamma_\nu) \, w_i^\nu \psi_N + ...
\end{aligned} \tag{24}$$

We have only displayed the leading order terms, the dots denote terms with more derivatives or insertions of the light quark mass matrix. It is understood that they are included up to the order one is working in the ϵ-expansion. Following the conventions of SU(2) HBChPT in the spin 1/2 sector [4, 7], we have defined the following structures

$$\begin{aligned}
D_\mu^{ij} \, \psi_j^\nu &= \left(\partial_\mu \, \delta^{ij} + \Gamma_\mu^{ij}\right) \psi_j^\nu \\
\Gamma_\mu^{ij} &= \Gamma_\mu \, \delta^{ij} - \frac{i}{2} \, \epsilon^{ijk} \, Tr[\tau^k \, \Gamma_\mu]
\end{aligned}$$

[5] In order to take into account the isospin 3/2 property of $\Delta(1232)$ we supply the Rarita-Schwinger spinor with an additional isospin index i, subject to the subsidiary condition $\tau^i \, \psi_\mu^i(x) = 0$.

$$
\begin{aligned}
\Gamma_\mu &= \frac{1}{2}\left[u^\dagger, \partial_\mu u\right] - \frac{i}{2}u^\dagger(\mathbf{v}_\mu + \mathbf{a}_\mu)u - \frac{i}{2}u(\mathbf{v}_\mu - \mathbf{a}_\mu)u^\dagger \\
u_\mu^{ij} &= u_\mu \delta^{ij} - i\epsilon^{ijk} w_\mu^k \\
w_\mu^i &= \frac{1}{2} Tr\left[\tau^i u_\mu\right] \\
u_\mu &= i u^\dagger \nabla_\mu U u^\dagger \\
\nabla_\mu U &= \partial_\mu U - i(\mathbf{v}_\mu + \mathbf{a}_\mu)U + iU(\mathbf{v}_\mu - \mathbf{a}_\mu) \\
U &= u^2 = exp\left(\frac{i}{F_\pi}\vec{\tau}\cdot\vec{\pi}\right) \ , \qquad (25)
\end{aligned}
$$

where $\mathbf{v}_\mu$, $\mathbf{a}_\mu$ denote external vector, axial-vector fields.

The "light" degrees of freedom of the spin 3/2 field, which are retained in the effective low-energy theory, are identified as

$$
T_\mu^i(x) \equiv P_v^+ \ P_{(33)\mu\nu}^{3/2} \ \psi_i^\nu(x) \exp(iMv\cdot x) \qquad (26)
$$

where we have introduced a spin 3/2 projection operator for fields with *fixed velocity* v_μ

$$
P_{(33)\mu\nu}^{3/2} = g_{\mu\nu} - \frac{1}{3}\gamma_\mu\gamma_\nu - \frac{1}{3}\left(\not{v}\gamma_\mu v_\nu + v_\mu\gamma_\nu \ \not{v}\right). \qquad (27)
$$

The remaining components,

$$
G_\mu^i(x) = \left(g_{\mu\nu} - P_v^+ \ P_{(33)\mu\nu}^{3/2}\right)\psi_i^\nu(x) \exp(iMv\cdot x), \qquad (28)
$$

are shown to be "heavy" [12, 13] and are integrated out.

Rewriting the lagrangians of Eq.(23) in terms of the spin 3/2 heavy baryon components T_μ and G_μ, and the corresponding "light" and "heavy" spin 1/2 components N, h, defined as

$$
\begin{aligned}
N(x) &= P_v^+ \ \psi_N \exp(iMv\cdot x) \\
h(x) &= P_v^- \ \psi_N \exp(iMv\cdot x), \qquad (29)
\end{aligned}
$$

the general lagrangians take the form

$$
\begin{aligned}
L_N &= \bar{N}\mathcal{A}_N N + \left(\bar{h}\mathcal{B}_N N + h.c.\right) - \bar{h}\mathcal{C}_N h \\
L_{\Delta N} &= \bar{T}\mathcal{A}_{\Delta N} N + \bar{G}\mathcal{B}_{\Delta N} N + \bar{h}\mathcal{D}_{N\Delta} T + \bar{h}\mathcal{C}_{N\Delta} G + h.c. \\
L_\Delta &= \bar{T}\mathcal{A}_\Delta T + \left(\bar{G}\mathcal{B}_\Delta T + h.c.\right) - \bar{G}\mathcal{C}_\Delta G. \qquad (30)
\end{aligned}
$$

Matrices $\mathcal{A}$, $\mathcal{B}$, $\mathcal{C}$ admit a low energy scale expansion–$\mathcal{A}$, $\mathcal{B}$ start at order ϵ^1, whereas $\mathcal{C}$ has a leading term of order 1. This allows to perform a systematic 1/M-expansion, following an approach developed by Mannel et al. in the field of heavy quark physics [31] , which was later applied to spin 1/2 HBChPT by Bernard et al. [8]. The result of this procedure is the effective action for the coupled $N\Delta$-system [12, 13]

$$S_{\text{eff}} = \int d^4x \left\{ \bar{T} \tilde{\mathcal{A}}_\Delta T + \bar{N} \tilde{\mathcal{A}}_N N + \left[\bar{T} \tilde{\mathcal{A}}_{\Delta N} N + h.c. \right] \right\} \tag{31}$$

with

$$\begin{aligned} \tilde{\mathcal{A}}_\Delta &= \mathcal{A}_\Delta + \gamma_0 \tilde{\mathcal{D}}^\dagger_{N\Delta} \gamma_0 \tilde{\mathcal{C}}_N^{-1} \tilde{\mathcal{D}}_{N\Delta} + \gamma_0 \mathcal{B}^\dagger_\Delta \gamma_0 \mathcal{C}_\Delta^{-1} \mathcal{B}_\Delta \\ \tilde{\mathcal{A}}_N &= \mathcal{A}_N + \gamma_0 \tilde{\mathcal{B}}^\dagger_N \gamma_0 \tilde{\mathcal{C}}_N^{-1} \tilde{\mathcal{B}}_N + \gamma_0 \mathcal{B}^\dagger_{\Delta N} \gamma_0 \mathcal{C}_\Delta^{-1} \mathcal{B}_{\Delta N} \\ \tilde{\mathcal{A}}_{\Delta N} &= \mathcal{A}_{\Delta N} + \gamma_0 \tilde{\mathcal{D}}^\dagger_{N\Delta} \gamma_0 \tilde{\mathcal{C}}_N^{-1} \tilde{\mathcal{B}}_N + \gamma_0 \mathcal{B}^\dagger_\Delta \gamma_0 \mathcal{C}_\Delta^{-1} \mathcal{B}_{\Delta N} \end{aligned} \tag{32}$$

and

$$\begin{aligned} \tilde{\mathcal{C}}_N &= \mathcal{C}_N - \mathcal{C}_{N\Delta} \mathcal{C}_\Delta^{-1} \gamma_0 \mathcal{C}^\dagger_{N\Delta} \gamma_0 \\ \tilde{\mathcal{B}}_N &= \mathcal{B}_N + \mathcal{C}_{N\Delta} \mathcal{C}_\Delta^{-1} \mathcal{B}_{\Delta N} \\ \tilde{\mathcal{D}}_{N\Delta} &= \mathcal{D}_{N\Delta} + \mathcal{C}_{N\Delta} \mathcal{C}_\Delta^{-1} \mathcal{B}_\Delta . \end{aligned} \tag{33}$$

The vertices relevant for our calculation can be read off directly from Eq.(31). Further analysis below will be divided into two classes of contributions, one-loop graphs and Born graphs. As one can see from Eq.(31), any calculation at $\mathcal{O}(\epsilon^3)$ which has a nucleon in the initial (and final) state, *completely* contains a $\mathcal{O}(p^3)$ calculation in the formalism of [8]. Furthermore, it shows unambiguously, which additional diagrams involving $\Delta(1232)$ must be appended.

3.1 Loop Graphs

To order ϵ^3, only one-loop graphs with vertices of order ϵ must be considered. Thus, the pieces in Eq.(31) we need are $\mathcal{A}_N^{(1)}$, $\mathcal{A}_\Delta^{(1)}$ and $\mathcal{A}_{\Delta N}^{(1)}$. More explicitly, these are found as

$$\begin{aligned} \mathcal{A}_N^{(1)} &= iv \cdot D + g_A \, S \cdot u \\ \mathcal{A}_{\Delta N}^{(1)} &= g_{\pi N \Delta} w_\mu^i \\ \mathcal{A}_\Delta^{(1)} &= - \left[i \, v \cdot D^{ij} - \Delta \, \delta^{ij} + g_1 \, S \cdot u^{ij} \right] \, g_{\mu\nu} \end{aligned} \tag{34}$$

where S_μ denotes the Pauli-Lubanski spin vector [7]. From matrices $\mathcal{A}_N^{(1)}$ and $\mathcal{A}_\Delta^{(1)}$ we determine the SU(2) HBChPT propagators in momentum space with soft momentum[6] $r_\mu = p_\mu - M v_\mu$:

$$\begin{aligned} S^{1/2}(v\cdot r) &= \frac{i}{v\cdot r + i\eta} \\ S^{3/2}_{\mu\nu}(v\cdot r) &= \frac{-\,i\,P^{3/2}_{\mu\nu}}{v\cdot r - \Delta + i\eta}\,\xi^{ij}_{I=3/2}\,, \end{aligned} \tag{35}$$

with $P^{3/2}_{\mu\nu}$ denoting the spin 3/2 HBChPT projector in d-dimensions [13]

$$P^{3/2}_{\mu\nu} = g_{\mu\nu} - v_{\mu\nu} + \frac{4}{d-1}\,S_\mu S_\nu \tag{36}$$

and

$$\xi^{ij}_{I=3/2} = \delta^{ij} - \frac{1}{3}\,\tau^i\tau^j \tag{37}$$

being the corresponding isospin 3/2 projector. From Eq.(35) one can see that the delta propagator counts as a quantity of order ϵ^{-1} in our expansion scheme.

At present, we have no systematic determination of the coupling constant $g_{\pi N\Delta}$ within the small scale expansion. For the time being we rely on the phenomenological analysis of Davidson, Mukhopadhyay and Wittman (DMW) [32], yielding

$$g^{HHK}_{\pi N\Delta} = \frac{F_\pi}{m_\pi}\,g^{DMW}_{\pi N\Delta} \approx 1.5\ \pm 0.2\,. \tag{38}$$

Finally, choosing the velocity vector $v_\mu = (1,0,0,0)$ and working in the Coulomb gauge $v\cdot\epsilon = v\cdot\epsilon' = 0$, we conclude that we have to calculate 18 loop diagrams, displayed in Fig. 3 and Fig. 4. Details of the calculation are given in Appendices B and C, the results will be discussed in section 4.

[6]Working to $\mathcal{O}(\epsilon^3)$ and in the absence of any $\mathcal{O}(\epsilon)$ Born diagrams due to our choice of gauge, we always can identify the large mass M with the physical mass of the nucleon M_N. Mass renormalization only becomes important in an $\mathcal{O}(\epsilon^4)$ HBChPT calculation of Compton scattering.

vertex	lagrangian
O(ϵ) γNN	$\mathcal{A}_N^{(1)} \to 0$ in Coulomb gauge
O(ϵ) $\gamma N\Delta$	$--$
O(ϵ^2) γNN	$\mathcal{A}_N^{(2)}$ and $\gamma_0 \mathcal{B}_N^{(1)\,\dagger} \gamma_0 \mathcal{C}_N^{(0)\,-1} \mathcal{B}_N^{(1)}$
O(ϵ^2) $\gamma\Delta N$	$\mathcal{A}_{\Delta N}^{(2)}$
O(ϵ^2) $\gamma\gamma NN$	$\gamma_0 \mathcal{B}_N^{(1)\,\dagger} \gamma_0 \mathcal{C}_N^{(0)\,-1} \mathcal{B}_N^{(1)}$
O(ϵ^3) $\gamma\gamma NN$	$\gamma_0 \mathcal{B}_N^{(2)\,\dagger} \gamma_0 \mathcal{C}_N^{(0)\,-1} \mathcal{B}_N^{(1)}$ + h.c.

Table 1: Vertices for Born graphs in Forward Compton Scattering

3.2 Born graphs

The Born graphs contributing at $\mathcal{O}(\epsilon^3)$ Compton scattering are shown in Figs. 1 and 2, with the pertinent vertices given in Table 1. The structures not involving the delta resonance can be taken from ref. [9][7]. We note that our use of the Coulomb gauge dramatically reduces the number of diagrams. Also, the possible diagram of Fig. 2.1d with an anomalous $\pi^0 \to \gamma\gamma$ vertex does not contribute in forward direction. Due to the fact that the photo-excitations of $\Delta(1232)$ begin with the M1 transition, there exists no $\gamma N\Delta$ vertex at $\mathcal{O}(\epsilon)$. Consequently, there is no 1/M-corrected interaction of this type at $\mathcal{O}(\epsilon^2)$ in Table 1. However, the relativistic counterterm lagrangian [12, 32]

$$\mathcal{L}_{c.t.}^{N\Delta} = \frac{ib_1}{2M_N} \bar{\psi}_i^\mu \left(g_{\mu\nu} + y\gamma_\mu\gamma_\nu\right) \gamma_\rho\gamma_5 \, \frac{1}{2} \, Tr\left[f_+^{\rho\nu} \, \tau^i\right] \psi_N, \tag{39}$$

provides the M1 $\gamma N\Delta$ transition strength and leads to an $\mathcal{O}(\epsilon^2)$ structure:

$$\mathcal{A}_{\Delta N}^{(2)} = \frac{ib_1}{M_N} S_\nu \, \frac{1}{2} \, Tr\left[f_+^{\nu\lambda} \, \tau^i\right], \tag{40}$$

with the chiral field tensor being defined as [7]

$$f_{\mu\nu}^{\pm} = u^\dagger \, F_{\mu\nu}^R \, u \, \pm \, u \, F_{\mu\nu}^L \, u^\dagger$$

[7] In general this is not the case. As will be shown in [13] the "heavy components" of the relativistic spin 3/2 field modify the counterterms of the NN lagrangian starting at $\mathcal{O}(\epsilon^2)$. In our specific case the NN vertices are unchanged.

$$F_{\mu\nu}^{L,R} = \partial_\mu F_\nu^{L,R} - \partial_\nu F_\mu^{L,R} - i \left[F_\mu^{L,R} , F_\nu^{L,R} \right]$$
$$F_\mu^R = \mathbf{v}_\mu + \mathbf{a}_\mu, \quad F_\mu^L = \mathbf{v}_\mu - \mathbf{a}_\mu \, . \tag{41}$$

We note that the off-shell parameter y in Eq.(39) does not contribute at order ϵ^2 when going to the effective heavy baryon lagrangian–it will only enter at $\mathcal{O}(\epsilon^3)$. However, since the Delta propagator Eq.(35) counts as order ϵ^{-1}, and we effectively have no $\mathcal{O}(\epsilon)$ vertices around, we do not have to consider ϵ^3 γNN or $\gamma N\Delta$ vertices to the order we are working. Furthermore, the absence of an $\mathcal{O}(\epsilon)$ $\gamma N\Delta$ vertex is also responsible for the fact that the $\mathcal{O}(\epsilon^3)$ two-photon seagull term does not get renormalized by Delta interactions. The only Born diagrams involving $\Delta(1232)$ are therefore s- and u-channel resonance exchange with vertices from $\mathcal{A}_{\Delta N}^{(2)}$ (diagrams 2.2a,b in Figure 2). At present, the magnitude of the finite $\mathcal{O}(\epsilon^2)$ counterterm b_1 is not known very accurately. Until one has identified a suitable b_1 dependent observable which has both been calculated in the small scale expansion and been reasonably well measured[8], we will employ a phenomenological relation found in ref. [32], which in our convention reads

$$b_1 \approx -\, 2.3 \, \frac{m_\pi}{2F_\pi} \, g_{\pi N\Delta}^{HHK} \approx -\, (\, 2.5 \, \pm \, 0.35 \,). \tag{42}$$

For the numerical estimate we have used $g_{\pi N\Delta}^{HHK}$ of Eq.(38). This completes the background necessary for the present application.

4 Forward Compton Scattering and Nucleon Polarizabilities

Having outlined our formalism, in this section we investigate the influence of the $\Delta(1232)$ resonance on the nucleon polarizabilities. We restrict ourselves to the case of forward scattering, which provides information on the electric polarizability $\bar{\alpha}_E$, the magnetic polarizability $\bar{\beta}_M$ and the spin polarizability γ. As mentioned above, for the spin-averaged quantities $\bar{\alpha}_E$ and $\bar{\beta}_M$ the results involving only nucleon and pion degrees of freedom are already known to $\mathcal{O}(p^4)$ [20] in the chiral expansion. Here we present a systematic analysis of

[8]Work along these lines is under way; V. Bernard, T.R. Hemmert, J. Kambor and U.-G. Meißner, in preparation.

the $\Delta(1232)$ contributions to $\bar{\alpha}_E$, $\bar{\beta}_M$ and γ at $\mathcal{O}(\epsilon^3)$. A complete calculation of all polarizabilities at $\mathcal{O}(\epsilon^4)$ including pion, nucleon and Delta degrees of freedom will be the subject of future work.

4.1 Spin-averaged Forward Compton Scattering

Working in the gauge—$\epsilon \cdot v = 0$—the spin-averaged Compton tensor in forward direction $\Theta_{\mu\nu}$ can be written as

$$\begin{aligned} \epsilon'^{\,\mu}\, \Theta_{\mu\nu}\, \epsilon^{\nu} &= e^2\, \epsilon'^{\,\mu} \epsilon^{\nu} \frac{1}{2} Tr\left[\, P_v^+\, T_{\mu\nu}(v,k)\,\right] \\ &= e^2\left[\, \epsilon' \cdot \epsilon\, U(\omega) \;+\; \epsilon' \cdot k\, \epsilon \cdot k\, V(\omega)\right] \,, \end{aligned} \tag{43}$$

where k is the four-momentum of a photon with energy $\omega = k{\cdot}v$. ϵ (ϵ') refer to the polarization vector of the incoming (outgoing) forward scattering photon and $T_{\mu\nu}(v,k)$ is the Fourier-transformed matrix element of two time-ordered electromagnetic currents

$$T_{\mu\nu}(v,k) = \int d^4x\, e^{ik\cdot x} \langle N(v)|\, T\left[\, J_\mu^{em}(x) J_\nu^{em}(x)\,\right] |N(v)\rangle \tag{44}$$

In the spin-averaged case all the information about the low-energy structure of the photon is contained in just two functions[9]– $U(\omega), V(\omega)$. However, there exists a structure-independent constraint [22] with respect to $U(\omega)$, stating that in the limit of zero photon energy one has to obtain the Thomson result of Eq.(1)

$$U(0) = Z^2/M \,, \tag{45}$$

where Z refers to the charge number of the Compton target and M is its mass. Furthermore, $U(\omega)$ has to be even under crossing symmetry[10], *i.e.* $U(\omega) = U(-\omega)$.

Keeping these two non-trivial constraints in mind we split up the calculation of $U(\omega),\ V(\omega)$ into four separate components:

$$\begin{aligned} U(\omega) &= U_N(\omega)^{Born} + U_N(\omega)^{loops} + U_\Delta(\omega)^{Born} + U_\Delta(\omega)^{loops} \\ V(\omega) &= V_N(\omega)^{Born} + V_N(\omega)^{loops} + V_\Delta(\omega)^{Born} + V_\Delta(\omega)^{loops} \end{aligned} \tag{46}$$

[9]The auxiliary function $V(\omega)$ can be eliminated for real photons. Nevertheless one can obtain information about the magnetic polarizability β from it.

[10]$U(\omega)$ is related to the function $f_1(\omega)$ of Eq.(15) via $f_1(\omega) = -\frac{e^2}{4\pi}\, U(\omega)$.

We start with the calculation of the nucleon Born contributions to $U(\omega)$, $V(\omega)$. In the Coulomb gauge $\epsilon \cdot v = 0$ there exist non-zero contributions at $\mathcal{O}(\epsilon^2)$ and $\mathcal{O}(\epsilon^3)$, as shown by the diagrams in Figures 1 and 2. To $\mathcal{O}(\epsilon^3)$ we find

$$\begin{aligned} U_N(\omega)^{Born} &= \frac{1}{M_N}\,\frac{1}{2}(1+\tau_3) \\ V_N(\omega)^{Born} &= \frac{1}{M_N^2\omega}\,\frac{1}{2}(1+\tau_3), \end{aligned} \tag{47}$$

with $U_N(\omega)$ solely stemming from the $\mathcal{O}(\epsilon^2)$ seagull diagram of Figure 1 and $V_N(\omega)$ arising from diagrams 2.1a and 2.1b of Figure 2. We also note that $U_N(0)^{Born}$ satisfies the Thomson limit Eq.(45) for proton ($Z = 1$) and neutron ($Z = 0$) targets, as expected. We therefore conclude that

$$U_N(0)^{loops} = U_\Delta(0)^{Born} = U_\Delta(0)^{loops} = 0\,, \tag{48}$$

and this will serve as a powerful constraint and check on our calculation.

The $\mathcal{O}(\epsilon^3)$ nucleon loop contributions to the spin-averaged functions can be obtained from the nine diagrams shown in Fig. 3 yielding[11], as detailed in Appendix B

$$\begin{aligned} U_N(\omega)^{loops} &= -\frac{11 g_A^2 \omega^2}{192\pi F_\pi^2 m_\pi} + \mathcal{O}(\omega^4) \\ V_N(\omega)^{loops} &= -\frac{g_A^2}{192\pi F_\pi^2 m_\pi} + \mathcal{O}(\omega^2) \end{aligned} \tag{49}$$

Note that the loop effects are isospin-independent (*i.e.* identical for neutron and proton) to this order. We have also checked that $U_N(\omega = 0)^{loops} = 0$ (Eq.(48)), by carefully analyzing the dimensionality dependence of the nine loop amplitudes as given in Appendix B.

Next, we evaluate $\Delta(1232)$ Born contributions to $U(\omega)$, $V(\omega)$. At $\mathcal{O}(\epsilon^3)$ we find two contributing diagrams, as shown in Fig. 2. They yield

$$\begin{aligned} U_\Delta(\omega)^{Born} &= -\frac{8 b_1^2 \omega^2}{9 M_N^2}\frac{\Delta}{\Delta^2 - \omega^2} \\ V_\Delta(\omega)^{Born} &= -\frac{8 b_1^2}{9 M_N^2}\frac{\Delta}{\Delta^2 - \omega^2} \end{aligned} \tag{50}$$

[11] Eq.(49) agrees with the $\mathcal{O}(p^3)$ result of [8].

where b_1 is the M1 $\Delta N\gamma$ coupling of Eq.(39). Again, the Thomson constraint $U_\Delta(0)^{Born} = 0$ holds, as required by Eq.(48).

Finally, the corresponding delta loop contributions can be found from the nine diagrams shown in Figure 4. Analyzing the invariant amplitudes given in Appendix C, we find

$$\begin{aligned} U_\Delta(\omega)^{loop} &= -\frac{g_{\pi N\Delta}^2\omega^2}{54\pi^2 F_\pi^2}\left[\frac{9\Delta}{\Delta^2-m_\pi^2} - \frac{9m_\pi^2}{(\Delta^2-m_\pi^2)^{3/2}}\log R + \frac{2}{\sqrt{\Delta^2-m_\pi^2}}\log R\right] \\ &\quad + \mathcal{O}(\omega^4) \\ V_\Delta(\omega)^{loop} &= -\frac{g_{\pi N\Delta}^2}{54\pi^2 F_\pi^2}\frac{1}{\sqrt{\Delta^2-m_\pi^2}}\log R + \mathcal{O}(\omega^2)\,, \end{aligned} \tag{51}$$

with R defined as

$$R = \frac{\Delta}{m_\pi} + \sqrt{\frac{\Delta^2}{m_\pi^2} - 1}. \tag{52}$$

Again we note the validity of the Thomson stricture $U_\Delta(\omega=0)^{loops} = 0$.

In order to extract the nucleon electric and magnetic polarizabilities, we now define the nucleon Born term subtracted quantities $\hat{U}(\omega), \hat{V}(\omega)$

$$\hat{U}(\omega) = U(\omega) - U_N(\omega)^{Born} \tag{53}$$
$$\hat{V}(\omega) = V(\omega) - V_N(\omega)^{Born} \tag{54}$$

and make the connections

$$\bar{\alpha}_E + \bar{\beta}_M = -\frac{e^2}{8\pi}\frac{\partial^2}{\partial\omega^{\,2}}\hat{U}(\omega)|_{\omega=0} \tag{55}$$
$$\bar{\beta}_M = -\frac{e^2}{4\pi}\hat{V}(\omega=0) \tag{56}$$

Adding up all three contributions[12] one finds $\bar{\alpha}_E$ and $\bar{\beta}_M$ to $\mathcal{O}(\epsilon^3)$:

$$\begin{aligned}
\bar{\alpha}_E &= +\frac{e^2}{4\pi}\,\frac{5g_A^2}{96\pi F_\pi^2}\,\frac{1}{m_\pi} \\
&\quad + 0 \\
&\quad + \frac{e^2}{4\pi}\,\frac{g_{\pi N\Delta}^2}{54\pi F_\pi^2}\,\frac{1}{\pi}\left[\,\frac{9\Delta}{\Delta^2-m_\pi^2}+\,\frac{\Delta^2-10m_\pi^2}{(\Delta^2-m_\pi^2)^{3/2}}\,\log R\,\right] \qquad (57) \\
&= [12.2\ (\text{N-loop}) +\ 0\ (\text{delta-pole}) +\ 8.6\ (\text{delta-loop})]\ \times 10^{-4}\ \text{fm}^3 \\
\bar{\beta}_M &= +\frac{e^2}{4\pi}\,\frac{g_A^2}{192\pi F_\pi^2}\,\frac{1}{m_\pi} \\
&\quad + \frac{e^2}{4\pi}\,\frac{8\ b_1^2}{9\ M_N^2}\,\frac{1}{\Delta} \\
&\quad + \frac{e^2}{4\pi}\,\frac{g_{\pi N\Delta}^2}{54\pi F_\pi^2}\,\frac{1}{\sqrt{\Delta^2-m_\pi^2}}\,\frac{1}{\pi}\log R \qquad (58) \\
&= [1.2\ (\text{N-loop}) +\ 12\ (\text{delta-pole}) +\ 1.5\ (\text{delta-loop})]\ \times 10^{-4}\ \text{fm}^3
\end{aligned}$$

In assessing these results, we observe that from the delta pole terms there exists a significant contribution to the magnetic polarizability but none to the corresponding electric polarizability at this order ! The strong effect on $\bar{\beta}_M$ is not surprising, as the large M1 nucleon-delta coupling is known to contribute substantially to the magnetic polarizability [17, 21]. Also, we note that at $\mathcal{O}(\epsilon^3)$ the $\Delta\pi$-loop contributions to $\bar{\beta}_M$ are of the same size as the $N\pi$-loop effects, which is unexpected. Furthermore, and perhaps most surprisingly, we find a large $\Delta\pi$-loop component in $\bar{\alpha}_E$! Even though the numerical values of the delta contributions in Eqs.(57,58) are understood to have sizable error bars due to quadratic dependence on the presently poorly known couplings $g_{\pi N\Delta}$ and b_1, it is clear that one cannot expect to achieve agreement with experiment at this order of the calculation–the effects of $\Delta(1232)$ are sizable and strongly renormalize the $N\pi$-loop results. In the $\mathcal{O}(p^4)$ calculation of [20] it has been shown that the large delta pole-contribution in $\bar{\beta}_M$ cancels

[12]The $N\pi$-loop parts of Eqs.(57,58) agree with the $\mathcal{O}(p^3)$ calculation of [8]. In SU(3) an estimate of spin 3/2 contributions to $\bar{\alpha}_E$ and $\bar{\beta}_M$ was given in [11]. $\bar{\alpha}_E$ and $\bar{\beta}_M$ have also been calculated in SU(2) relativistic baryon ChPT [33].

to a large extent against $N\pi$-loop effects at that order. In addition to the simple delta poles the counterterms of BKSM have been determined via "resonance saturation". The large $\Delta\pi$-loop effects that we find at $\mathcal{O}(\epsilon^3)$ are therefore not accounted for[13] in the counterterms of [20] ! Unless one finds a cancelation through $\Delta\pi$-loops in a future $\mathcal{O}(\epsilon^4)$ calculation, one would have to conclude that "resonance saturation" via simple pole-graphs is highly suspect for counterterms in the baryon sector[14]. Future work will address this important question. Finally, we note that the results for $\bar{\alpha}_E$ and $\bar{\beta}_M$ are isospin independent at $\mathcal{O}(\epsilon^3)$. The surprising experimental results $\bar{\alpha}_E^n > \bar{\alpha}_E^p$, $\bar{\beta}_E^n > \bar{\beta}_E^p$ cannot be addressed at this order and also warrant an investigation at sub-leading order.

In order to obtain an estimate of the convergence of the perturbation series and to check the field-theoretic consistency of our calculation, it is useful to perform a chiral expansion of our results for the polarizabilities, yielding

$$\begin{aligned}
\bar{\alpha}_E^\chi &= +\frac{e^2}{4\pi}\,\frac{1}{6\pi F_\pi^2}\,\frac{1}{m_\pi}\Big\{\frac{5g_A^2}{16}+\frac{g_{\pi N\Delta}^2}{\pi}\frac{m_\pi}{\Delta}\left[1+\frac{1}{9}\log\left(\frac{2\Delta}{m_\pi}\right)\right] \\
&\qquad +O\left(\frac{m_\pi^3}{\Delta^3}\right)\Big\} \qquad (59)\\
\bar{\beta}_M^\chi &= +\frac{e^2}{4\pi}\,\frac{1}{6\pi F_\pi^2}\,\frac{1}{m_\pi}\Big\{\frac{g_A^2}{32}+\frac{m_\pi}{\Delta}\left[\frac{b_1^2}{3\pi}\frac{(4\pi F_\pi)^2}{M_N^2}+\frac{g_{\pi N\Delta}^2}{9\pi}\log\left(\frac{2\Delta}{m_\pi}\right)\right] \\
&\qquad +O\left(\frac{m_\pi^3}{\Delta^3}\right)\Big\} \qquad (60)
\end{aligned}$$

We note that the long-range pion cloud, which scales as $1/m_\pi$, provides the dominant singularity in the chiral limit, as expected. Also, one can see that decoupling of the delta resonance in the chiral limit is manifest. Finally, we note that the leading order p^4-terms in the chiral expansion of the $\Delta\pi$-loop contributions is already a good approximation to the full order ϵ^3 expressions. The contributions to $\bar{\alpha}_E$ and $\bar{\beta}_M$ are thereby changed by 15 and 7 % respectively, indicating that the bulk of the effects due to $\Delta(1232)$

[13] In particular, the counterterm contribution to $\bar{\alpha}_E$ has been estimated to be $\delta\alpha \approx 2.0 \times 10^{-4}$ fm^3 [20] !

[14] Of course these counterterms can still be determined from other experiments. A breakdown of the "resonance saturation" hypothesis only means that the numerical value of the counterterms cannot be understood within a simple resonance *model*.

are obtained at order p^4 in the chiral expansion ! Of course we emphasize that these considerations are only an *indication* of what might happen at the next order, future work will address these issues. We now move on to discuss the case of spin-dependent quantities in Compton scattering.

4.2 Spin-dependent Forward Compton Scattering

In the presence of spin-dependence the Compton tensor for forward scattering of real photons Eq.(43) from a spin 1/2 particle has to be expanded by extra (spin-dependent) structures. Choosing $v_\mu = (1,0,0,0)$ and again working in Coulomb gauge $\epsilon \cdot v = \epsilon' \cdot = 0$ we can write

$$\begin{aligned} \epsilon'^{\,\mu}\, \Theta_{\mu\nu}\, \epsilon^\nu \;\; = \;\; & e^2 \Big[\;\; - \;\; \hat{\epsilon}' \cdot \hat{\epsilon}\, U(\omega) \;\; + \;\; \hat{\epsilon}' \cdot \vec{k}\, \hat{\epsilon} \cdot \vec{k}\, V(\omega) \\ & + i\, \omega\, W^{(1)}(\omega)\, \vec{\sigma} \cdot (\hat{\epsilon}' \times \hat{\epsilon}) + i\, \omega\, W^{(2)}(\omega)\, \hat{\epsilon} \cdot \vec{k}\, \vec{\sigma} \cdot \left(\hat{\epsilon}' \times \vec{k} \right) \\ & + i\, \omega\, W^{(3)}(\omega)\, \hat{\epsilon}' \cdot \vec{k}\, \vec{\sigma} \cdot \left(\hat{\epsilon} \times \vec{k} \right) \Big] \;\; , \end{aligned} \tag{61}$$

where $\omega = v \cdot k$ denotes the energy of the forward scattering photon with four-momentum k_μ. In the following we enforce the transversality condition $\hat{\epsilon} \cdot \vec{k} = \hat{\epsilon}' \cdot \vec{k} = 0$ and therefore only work with the auxiliary function[15] $W^{(1)}(\omega)$, which contains the information about the spin 1/2 structure of the target nucleon. Having factored out an extra ω, we note that $W^{(1)}(\omega)$ is even under crossing (i.e. $W^{(1)}(\omega) = W^{(1)}(-\omega)$) and receives contributions from four different sources, analogously to Eq.(46):

$$W^{(1)}(\omega) = W_N^{(1)}(\omega)^{Born} + W_N^{(1)}(\omega)^{loops} + W_\Delta^{(1)}(\omega)^{Born} + W_\Delta^{(1)}(\omega)^{loops} \tag{62}$$

First we calculate the nucleon Born contributions to $W^{(1)}(\omega)$. They arise at at $\mathcal{O}(\epsilon^3)$ from the four diagrams 2.1a-d in Figure 2. One finds

$$W_N^{(1)}(\omega)^{Born} = -\frac{1}{4M_N^2} \, \Big\{ \kappa_p^2 \;\; (1+\tau_3) \;\; + \;\; \kappa_n^2 \;\; (1-\tau_3) \Big\} \;\; , \tag{63}$$

where $\kappa_{p,(n)}$ corresponds to the anomalous magnetic moment for a proton (neutron) target. As noted before, the contribution from the anomalous

[15] From $W^{(2)}(\omega)$ and $W^{(3)}(\omega)$ one can obtain the third-order spin polarizabilities γ_3, γ_4 of ref. [34]. However, we relegate this analysis to future work where we will study the complete set of third-order spin polarizabilities of the nucleon.

process $\pi^0 \to \gamma\gamma$ (diagram 2.1d in Figure 2) vanishes in the forward direction. However, the sum of the other three diagrams satisfies the famous LET due to Gell-Mann, Goldberger and Low [22], with the two-photon seagull diagram 2.1c arising from $1/M^2$ corrections (see Table 1) playing a pivotal role. Relating $W_N^{(1)}(\omega)^{Born}$ of Eq.(63) to the function $f_2(\omega)$ of Eq.(15) via $f_2(\omega) = e^2/4\pi\ W^{(1)}(\omega)$, one finds in the limit of zero photon energy

$$f_2(0) = -\ \frac{e^2\ \kappa^2}{8\pi\ M_N^2} \tag{64}$$

Having satisfied the low energy constraint we conclude that

$$W_N^{(1)}(0)^{loop} = W_\Delta^{(1)}(0)^{Pole} = W_\Delta^{(1)}(0)^{loop} = 0\ , \tag{65}$$

which constitutes a non-trivial check on our calculations.

The $\mathcal{O}(\epsilon^3)$ $N\pi$-loop contribution to $W^{(1)}(\omega)$ can be obtained from just six diagrams (3a-3f) of Figure 3. With details of the calculation given in Appendix B we find[16]

$$W_N^{(1)}(\omega)^{loops} = \frac{g_A^2}{2F_\pi^2}\frac{\omega^2}{12\pi^2 m_\pi^2} +\ \mathcal{O}(\omega^4)\ , \tag{66}$$

so that the LET constraint $W_N^{(1)}(0)^{loop} = 0$ is satisfied.

The $\mathcal{O}(\epsilon^3)$ delta Born contributions to the spin-flip function $W^{(1)}(\omega)$ are given by diagrams 2.2a and 2.2b of Figure 2, yielding

$$W_\Delta^{(1)}(\omega)^{Born} = -\ \frac{4b_1^2}{9M_N^2}\ \frac{\omega^2}{\Delta^2 - \omega^2}\ . \tag{67}$$

Again, the LET stricture Eq.(65) holds explicitly.

Finally, the $\mathcal{O}(\epsilon^3)$ $\Delta\pi$-loop contributions to $W^{(1)}(\omega)$ arise from diagrams 4a-f in Figure 4. With details of the calculation given in Appendix C, we find

$$\begin{aligned} W_\Delta^{(1)}(\omega)^{loop} &= \frac{g_{\pi N\Delta}^2\ \omega^2}{54\pi^2\ F_\pi^2}\left[\frac{3m_\pi^2\Delta}{(\Delta^2 - m_\pi^2)^{5/2}}\log R - \frac{\Delta^2 + 2m_\pi^2}{(\Delta^2 - m_\pi^2)^2}\right] \\ &\quad + \mathcal{O}(\omega^4)\ , \end{aligned} \tag{68}$$

[16]Eq.(66) agrees with the $\mathcal{O}(p^3)$ result of [8].

where R has been defined in Eq.(52). The d-dependence of the pertinent amplitudes in Appendix C–induced by the spin 3/2 propagator of Eq.(35)– leads to a highly complex cancelation pattern among the diagrams, ultimately yielding $W_\Delta^{(1)}(0)^{loop} = 0$ as required by Eq.(65).

In analogy to the spin-independent discussion in section 4.1 we introduce the nucleon Born-term subtracted function

$$\hat{W}^{(1)}(\omega) = W^{(1)}(\omega) - W_N^{(1)}(\omega)^{Born} \tag{69}$$

and obtain the spin polarizability γ of the nucleon

$$\gamma = \frac{e^2}{8\pi}\,\frac{\partial^2}{\partial\omega^{\,2}}\hat{W}^{(1)}(\omega)|_{\omega=0}\;, \tag{70}$$

which was defined via Eq.(17).

Summing the three contributions[17] contained in $\hat{W}^{(1)}(\omega)$ one finds γ to $\mathcal{O}(\epsilon^3)$:

$$\begin{aligned}
\gamma^{O(\epsilon^3)} &= +\frac{e^2}{4\pi}\,\frac{g_A^2}{24\pi^2 F_\pi^2}\,\frac{1}{m_\pi^2} \\
&\quad -\frac{e^2}{4\pi}\,\frac{4b_1^2}{9M_N^2}\,\frac{1}{\Delta^2} \\
&\quad -\frac{e^2}{4\pi}\,\frac{g_{\pi N\Delta}^2}{54\pi^2 F_\pi^2}\left[\,\frac{\Delta^2+2m_\pi^2}{(\Delta^2-m_\pi^2)^2} - \frac{3m_\pi^2\Delta}{(\Delta^2-m_\pi^2)^{5/2}}\log R\,\right] \\
&= (4.5\ \text{(N-loop)} - 4.0\text{(delta-pole)} - 0.4\text{(delta-loop)}) \times 10^{-4}\ \text{fm}^4\;.
\end{aligned} \tag{71}$$

We note that as in the case of $\bar{\alpha}_E$ and $\bar{\beta}_M$ there is no isospin dependence at $\mathcal{O}(\epsilon^3)$. Also, $\Delta\pi$-loops are only playing a minor role in the spin polarizability at this order. Finally, the large positive contribution of the $N\pi$-loops is nearly completely canceled by the delta Born graphs. In the case of the spin polarizability we cannot yet make a direct experimental comparison, as explained in section 2. However, comparing with the sum rule value given in Eq.(18) we see that the $\Delta(1232)$ contribution goes in the right direction but is not large enough in (negative) magnitude in order to bring about experimental agreement. We also note that at present we do not have a $\mathcal{O}(p^4)$ calculation in HBChPT with which to compare. However, the one-loop

[17] Our findings agree with the $N\pi$- and $\Delta\pi$-loop results given in [8].

relativistic baryon results of Eq.(22) already give an indication that even if one extends the $O(p^3)$ HBChPT result of Eq.(21) to the next order, one will not be able to describe γ without keeping $\Delta(1232)$ as an explicit degree of freedom in the theory. Studying the chiral limit of the spin polarizability supports this viewpoint. We find

$$\gamma^{\chi} \;=\; \frac{e^2}{4\pi}\,\frac{1}{216\pi^2\,F_\pi^2}\,\frac{1}{m_\pi^2}\left[9g_A^2-6b_1^2\,\frac{(4\pi F_\pi)^2}{M_N^2}\,\frac{m_\pi^2}{\Delta^2}-4g_{\pi N\Delta}^2\,\frac{m_\pi^2}{\Delta^2}+\;\mathcal{O}\left(\frac{m_\pi^4}{\Delta^4}\right)\right] \tag{72}$$

One observes that the $1/m_\pi^2$ singularity due to the pion cloud of the nucleon remains leading in the chiral limit and that delta decoupling holds. We also note that the $\Delta\pi$-loop contributions increase in magnitude to $-0.6\ 10^{-4}$ fm^4 but remain small. Most importantly, Eq.(72) shows us that all delta effects only start contributing at $\mathcal{O}(p^5)$ (!) in standard SU(2) HBChPT. The spin dependent polarizability of the nucleon is therefore a prime example of how a theory with explicit delta degrees of freedom can dramatically improve the convergence of the perturbation series. In light of the cancelations in Eq.(71) we are encouraged that at $\mathcal{O}(\epsilon^4)$ one may be able to achieve a good understanding of the spin polarizability with the help of the small scale expansion[18].

4.3 Critical Discussion of $\mathcal{O}(\epsilon^3)$ Results

Before concluding it is useful to discuss some of the arguments of which we are aware why an $\mathcal{O}(\epsilon^3)$ calculation can perform poorly on the phenomenological side and on the other hand show all the correct field-theoretic constraints of LETs, heavy mass decoupling, correct chiral limit etc.

i) The heavy baryon propagator for nucleons of Eq.(35) receives "propagator corrections" via 1/M vertices in matrix $\tilde{\mathcal{A}}_N^{(2)}$ of Eq.(32), which in one-loop diagrams only begin to show up at $\mathcal{O}(\epsilon^4)$. From a relativistic viewpoint these $1/M$ corrections correspond to effects pertaining to the lower components of a Dirac spinor.

[18] There certainly have been many attempts in the literature to call the delta to the rescue in order to get reasonable numbers for the sum rules of Eq.(18). We emphasize again that our results in Eq.(71) follow from the *systematic small scale expansion in HBChPT*, as laid out in section 3.

ii) For the heavy baryon propagator of a spin 3/2 particle there are analogous $1/M$ induced propagator corrections in matrix $\tilde{\mathcal{A}}^{(2)}_{\Delta}$ of Eq.(32). In this case they have the additional effect of correcting the pure spin 3/2 projector of Eq.(35) by bringing in some information about the off-shell spin 1/2 components of a relativistic spin 3/2 particle. Phenomenologically it is well known that the spin 1/2 components of the relativistic spin 3/2 propagator can play an important effect in some observables [35]. Again, at the one-loop level these effects only start showing up at $\mathcal{O}(\epsilon^4)$.

iii) In $\mathcal{O}(\epsilon^3)$ calculations the incoming (and outgoing) soft momentum of the baryon is usually a higher order effect. Only at the next order does this momentum fully contribute and the size of these "recoil corrections" can be quite large for some observables.

iv) Isospin is usually not broken in calculations at the $\mathcal{O}(\epsilon^3)$ level which can be a problem in some cases.

v) Often one is calculating observables which are dominated by loop effects. Therefore one is only calculating the leading order of these observables, although technically one might have to work to third or fourth order in HBChPT. As experience from many calculations in the meson sector of ChPT teaches us, one should always consider the leading and the first (at least) non-leading order in an observable before one can try to judge the quality of a ChPT result.

This list is certainly not complete. The concerns raised are valid beyond our particular case of the $\mathcal{O}(\epsilon^3)$ calculation of the polarizabilities of the nucleon. In fact, most of these points also apply to SU(2) HBChPT without explicit delta degrees of freedom and "leading log" calculations in SU(3) HBChPT. For our particular case of interest—the polarizabilities of the nucleon—all of these points strongly suggest moving onto the $\mathcal{O}(\epsilon^4)$ calculation.

5 Conclusions

The Compton scattering process offers the opportunity to probe nucleon structure in a relatively clean fashion, via measurement of various "polarizabilities" which probe the nucleon response to quasi-static excitations. In particular recent years have seen the measurement of electric and magnetic polarizabilities for both neutron and proton and spin polarizability measure-

ments should be available by the millennium. On the theoretical side, $\mathcal{O}(p^3)$ predictions for $\bar{\alpha}_E$ and $\bar{\beta}_M$ within heavy baryon chiral perturbation theory give a surprisingly good picture of the experimental situation. However, corresponding predictions for the spin polarizability are not in good agreement with the values given from DHG sum rule arguments. When extended to $\mathcal{O}(p^4)$ reasonable agreement is obtained for $\bar{\alpha}_E$ and $\bar{\beta}_M$, but at the cost of considerable uncertainty associated with effects such as the $\Delta(1232)$, which is included only as a very heavy particle contributing to various counterterms. In this paper we have removed this obstacle by treating the $\Delta(1232)$ as a specific degree of freedom within the heavy baryon method. Our calculation was performed to $\mathcal{O}(\epsilon^3)$ where ϵ is taken as a soft momentum, as m_π or as the nucleon-delta mass difference. We find, perhaps not surprisingly, that inclusion of delta effects makes large changes to all three polarizabilities.

The good agreement with experiment at $\mathcal{O}(p^3)$ for $\bar{\alpha}_E$ and $\bar{\beta}_M$ is destroyed at $\mathcal{O}(\epsilon^3)$, whereas the spin polarizability γ improves dramatically when compared with currently available sum rule information. Furthermore, we have discussed consequences of our HBChPT results in the light of existing $\mathcal{O}(p^4)$ and relativistic one-loop calculations. Indeed, we regard our calculation as merely preliminary and look forward to extending this work to higher order.

A Loop Functions

We express the invariant amplitudes of Feynman diagrams containing pion-loops around a nucleon in terms of J-functions, defined via

$$\frac{1}{i}\int\frac{d^d\ell}{(2\pi)^d}\frac{\{1,\ell_\mu\ell_\nu,\ell_\mu\ell_\nu\ell_\alpha\ell_\beta\}}{(v\cdot\ell-\omega-i\epsilon)(m_\pi^2-\ell^2-i\epsilon)} = \{J_0(\omega,m_\pi^2), \quad (73)$$
$$g_{\mu\nu}J_2(\omega,m_\pi^2)+v_\mu v_\nu J_3(\omega,m_\pi^2),$$
$$(g_{\mu\nu}g_{\alpha\beta}+\text{perm.})J_6(\omega,m_\pi^2)+...\}$$

Employing the following identities

$$J_2\left(\omega,m_\pi^2\right) = \frac{1}{d-1}\left[\left(m_\pi^2-\omega^2\right)J_0\left(\omega,m_\pi^2\right)-\omega\,\Delta_\pi\right] \quad (74)$$

$$J_6\left(\omega,m_\pi^2\right) = \frac{1}{d+1}\left[\left(m_\pi^2-\omega^2\right)J_2\left(\omega,m_\pi^2\right)-\frac{m_\pi^2\omega}{d}\,\Delta_\pi\right], \quad (75)$$

one concludes that all loop-integrals can be expressed via the basis-function J_0. For the $N\pi$ loop-integrals we use [7]

$$J_0\left(\omega,m_\pi^2\right)=-4L\omega+\frac{\omega}{8\pi^2}\left(1-2\ln\frac{m_\pi}{\mu}\right)-\frac{1}{4\pi^2}\sqrt{m_\pi^2-\omega^2}\arccos\frac{-\omega}{m_\pi}, \quad (76)$$

whereas for the $\Delta\pi$ loop-integrals we employ the analytically continued function

$$J_0\left(\omega,m_\pi^2\right) = -4L\omega+\frac{\omega}{8\pi^2}\left(1-2\ln\frac{m_\pi}{\mu}\right)+\frac{1}{4\pi^2}\sqrt{\omega^2-m_\pi^2}$$
$$\times\log\left[-\frac{\omega}{m_\pi}+\sqrt{\frac{\omega^2}{m_\pi^2}-1}\right]. \quad (77)$$

In Eqs. (74), (75), (76) and (77) we have used the same conventions as [7],

$$\Delta_\pi = 2m_\pi^2\left(L+\frac{1}{16\pi^2}\ln\frac{m_\pi}{\mu}\right)+O\left(d-4\right),$$
$$L = \frac{\mu^{d-4}}{16\pi^2}\left[\frac{1}{d-4}+\frac{1}{2}\left(\gamma_E-1-\ln4\pi\right)\right], \quad (78)$$

where we introduced the Euler-Mascharoni constant, $\gamma_E = 0.557215$, and the scale μ in the dimensional regularization scheme we use for the evaluation of the integrals.

Finally, with J_i' and J_i'' we define the first and second partial derivative with respect to m_π^2,

$$J_i'\left(\omega, m_\pi^2\right) = \frac{\partial}{\partial\left(m_\pi^2\right)} J_i\left(\omega, m_\pi^2\right) , \tag{79}$$

$$J_i''\left(\omega, m_\pi^2\right) = \frac{\partial^2}{\partial\left(m_\pi^2\right)^2} J_i\left(\omega, m_\pi^2\right) . \tag{80}$$

B $N\pi$ Loops in Forward Compton Scattering

Using the J-function formalism defined in Appendix A and the lagrangians of Eq.(34) one can get exact solutions for the nine $N\pi$-loop diagrams of Figure 3. With ϵ_μ (ϵ'_μ) we denote the polarization four-vector of the incoming (outgoing) photon with constant four-momentum k_μ and energy ω. We find

$$\begin{aligned}
Amp^{N\pi}_{1+2} &= C\ \bar{u}(r)\Big\{ \ -\epsilon\cdot\epsilon'\left[J_0(\omega,m_\pi^2)+J_0(-\omega,m_\pi^2)\right] \qquad (81)\\
&\quad +2\ [S_\mu,S_\nu]\ \epsilon'^{\,\mu}\epsilon^\nu\left[J_0(\omega,m_\pi^2)-J_0(-\omega,m_\pi^2)\right]\Big\}\ u(r)\\
Amp^{N\pi}_{3..6} &= C\ \bar{u}(r)\Big\{ \ +4\ \epsilon\cdot\epsilon'\int_o^1 dx\left[J'_2(\omega x,m_\pi^2)+J'_2(-\omega x,m_\pi^2)\right] \qquad (82)\\
&\quad -8\ [S_\mu,S_\nu]\ \epsilon'^{\,\mu}\epsilon^\nu\int_o^1 dx\left[J'_2(\omega x,m_\pi^2)-J'_2(-\omega x,m_\pi^2)\right]\\
&\quad -2\ \epsilon\cdot k\ \epsilon'\cdot k\int_0^1 dx\ x(1-2x)\left[J'_0(\omega x,m_\pi^2)+J'_0(-\omega x,m_\pi^2)\right]\\
&\quad +2\ [S_\mu,S_\nu]\ \left(\epsilon'\cdot k\ k^\mu\epsilon^\nu+\epsilon\cdot k\ \epsilon'^{\,\mu}k^\nu\right)\int_0^1 dx\ x(1-2x)\\
&\qquad\qquad \times\left[J'_0(\omega x,m_\pi^2)-J'_0(-\omega x,m_\pi^2)\right]\Big\}\ u(r)\\
Amp^{N\pi}_{7+8} &= C\ \bar{u}(r)\Big\{ \ -4\ \epsilon\cdot\epsilon'\ (d+1)\int_o^1 dx\ (1-x)\\
&\qquad\qquad \times\left[J''_6(\omega x,m_\pi^2)+J''_6(-\omega x,m_\pi^2)\right] \qquad (83)\\
&\quad +4\ \epsilon\cdot\epsilon'\ \omega^2\int_o^1 dx\ (1-x)x^2\left[J''_2(\omega x,m_\pi^2)+J''_2(-\omega x,m_\pi^2)\right]\\
&\quad -\epsilon\cdot k\ \epsilon'\cdot k\int_0^1 dx\ (1-x)\left[8x(2x-1)+(2x-1)^2(d-1)\right]\\
&\qquad\qquad \times\left[J''_2(\omega x,m_\pi^2)+J''_2(-\omega x,m_\pi^2)\right]\\
&\quad +\epsilon\cdot k\ \epsilon'\cdot k\ \omega^2\int_0^1 dx\ (1-x)\ x^2\ (2x-1)^2\\
&\qquad\qquad \times\left[J''_0(\omega x,m_\pi^2)+J''_0(-\omega x,m_\pi^2)\right]\Big\}\ u(r)\\
Amp^{N\pi}_{9} &= C\ \bar{u}(r)\Big\{ \ +2\ \epsilon\cdot\epsilon'\ (d-1)\ J'_2(0,m_\pi^2)\Big\}\ u(r)\ , \qquad (84)
\end{aligned}$$

with the common factor

$$C = i\,\frac{e^2 g_A^2}{2F_\pi^2}\ ,$$

In order to evaluate the polarizabilities, we expand the nine amplitudes into a power series in ω and only keep the terms of interest:

$$\begin{aligned}
Amp_{1+2}^{N\pi} &= C\ \bar{u}(r)\Big\{\ +\ \epsilon\cdot\epsilon'\left[\frac{m_\pi}{4\pi} - \omega^2\,\frac{1}{8\pi m_\pi} + \mathcal{O}(\omega^4)\right] \qquad (85)\\
&\quad +\omega\ [S_\mu, S_\nu]\ \epsilon'^{\,\mu}\epsilon^{\nu}\ \Big[\ -\ \frac{1}{2\pi^2}\left(32\pi^2 L + 1 + 2\log\frac{m_\pi}{\lambda}\right)\\
&\quad\qquad + \omega^2\,\frac{1}{3\pi^2 m_\pi^2} + \mathcal{O}(\omega^4)\ \Big]\ \Big\}\ u(r)\\
Amp_{3..6}^{N\pi} &= C\ \bar{u}(r)\Big\{\ +\ \epsilon\cdot\epsilon'\left[-\frac{m_\pi}{2\pi} + \omega^2\,\frac{1}{12\pi m_\pi} + \mathcal{O}(\omega^4)\right] \qquad (86)\\
&\quad +\omega\ [S_\mu, S_\nu]\ \epsilon'^{\,\mu}\epsilon^{\nu}\ \Big[\ \frac{1}{2\pi^2}\left(\frac{96\pi^2}{(d-1)}L + \frac{5}{3} + 2\log\frac{m_\pi}{\lambda}\right)\\
&\quad\qquad - \omega^2\,\frac{1}{6\pi^2 m_\pi^2} + \mathcal{O}(\omega^4)\ \Big]\\
&\quad + \epsilon\cdot k\ \epsilon'\cdot k\left[-\frac{1}{24\pi m_\pi} + \mathcal{O}(\omega^4)\right]\\
&\quad + ...\Big\}\ u(r)\\
Amp_{7+8}^{N\pi} &= C\ \bar{u}(r)\Big\{\ +\ \epsilon\cdot\epsilon'\left[\frac{5m_\pi}{8\pi} - \omega^2\,\frac{5}{96\pi m_\pi} + \mathcal{O}(\omega^4)\right] \qquad (87)\\
&\quad + \epsilon\cdot\epsilon'\left[-\omega^2\,\frac{2}{96\pi m_\pi} + \mathcal{O}(\omega^4)\right]\\
&\quad + \epsilon\cdot k\ \epsilon'\cdot k\left[\frac{1}{32\pi m_\pi} + \mathcal{O}(\omega^2)\right]\\
&\quad + ...\Big\}\ u(r)\\
Amp_{9}^{N\pi} &= C\ \bar{u}(r)\Big\{\ +\ \epsilon\cdot\epsilon'\left[-\frac{3m_\pi}{8\pi}\right]\Big\}\ u(r) \qquad (88)
\end{aligned}$$

In section 4 we construct the auxiliary functions $U(\omega)$, $V(\omega)$ and $W(\omega)$ from Eqs.(85-88).

C $\Delta\pi$ Loops in Forward Compton Scattering

Using the same conventions as in Appendix B with a new overall factor

$$D = i\,\frac{4e^2 g_{\pi N\Delta}^2}{3F_\pi^2}\ ,$$

we find the invariant amplitudes for the nine diagrams of Figure 4:

$$\begin{aligned}
Amp_{1+2}^{\Delta\pi} &= D\ \bar{u}(r)\ \Big\{\ -\ \epsilon\cdot\epsilon'\ \frac{d-2}{d-1}\Big[J_0(\omega-\Delta,m_\pi^2)+J_0(-\omega-\Delta,m_\pi^2)\Big] \qquad (89)\\
&\quad -\ [S_\mu\ ,\ S_\nu]\ \epsilon'^\mu\epsilon^\nu\ \frac{2}{d-1}\Big[J_0(\omega-\Delta,m_\pi^2)-J_0(-\omega-\Delta,m_\pi^2)\Big]\ \Big\}\ u(r)\\
Amp_{3..6}^{\Delta\pi} &= D\ \bar{u}(r)\ \Big\{\ 4\ \epsilon\cdot\epsilon'\ \frac{d-2}{d-1}\int_0^1 dx\,\Big[J_2'(\omega x-\Delta,m_\pi^2)+J_2'(-\omega x-\Delta,m_\pi^2)\Big] \qquad (90)\\
&\quad +\ 4\ [S_\mu\ ,\ S_\nu]\ \epsilon'^\mu\epsilon^\nu\ \frac{2}{d-1}\int_0^1 dx\,\Big[J_2'(\omega x-\Delta,m_\pi^2)-J_2'(-\omega x-\Delta,m_\pi^2)\Big]\\
&\quad -\ 2\ \epsilon\cdot k\ \epsilon'\cdot k\ \frac{d-2}{d-1}\int_0^1 dx\ x(1-2x)\Big[J_0'(\omega x-\Delta,m_\pi^2)+J_0'(-\omega x-\Delta,m_\pi^2)\Big]\\
&\quad -\ [S_\mu\ ,\ S_\nu]\,(\epsilon'\cdot k\ k^\mu\epsilon^\nu+\epsilon\cdot k\ \epsilon'^\mu k^\nu)\ \frac{2}{d-1}\int_0^1 dx\ x(1-2x)\\
&\qquad\qquad \times\ \Big[J_0'(\omega x-\Delta,m_\pi^2)-J_0'(-\omega x-\Delta,m_\pi^2)\Big]\ \Big\}\ u(r)\\
Amp_{7+8}^{\Delta\pi} &= D\ \bar{u}(r)\ \Big\{\ -\ \epsilon\cdot\epsilon'\ 4\ \frac{(d-2)(d+1)}{(d-1)}\ \int_0^1 dx\ (1-x) \qquad (91)\\
&\qquad\qquad \times\ \Big[J_6''(\omega x-\Delta,m_\pi^2)+J_6''(-\omega x-\Delta,m_\pi^2)\Big]\\
&\quad +\ \epsilon\cdot\epsilon'\ \omega^2\ 4\ \frac{d-2}{d-1}\ \int_0^1 dx\ (1-x)\ x^2\Big[J_2''(\omega x-\Delta,m_\pi^2)+J_2''(-\omega x-\Delta,m_\pi^2)\Big]\\
&\quad -\ \epsilon\cdot k\ \epsilon'\cdot k\ \frac{d-2}{d-1}\ \int_0^1 dx\ (1-x)\ (2x-1)\ [8x+(2x-1)(d-1)]\\
&\qquad\qquad \times\ \Big[J_2''(\omega x-\Delta,m_\pi^2)+J_2''(-\omega x-\Delta,m_\pi^2)\Big]\\
&\quad +\ \epsilon\cdot k\ \epsilon'\cdot k\ \omega^2\ \frac{d-2}{d-1}\ \int_0^1 dx\ (1-x)\ x^2\ (2x-1)^2\\
&\qquad\qquad \times\ \Big[J_0''(\omega x-\Delta,m_\pi^2)+J_0''(-\omega x-\Delta,m_\pi^2)\Big]\ \Big\}\ u(r)\\
Amp_{9}^{\Delta\pi} &= D\ \bar{u}(r)\ \epsilon\cdot\epsilon'\ 2\ (d-2)\ J_2'(-\Delta,m_\pi^2)\ u(r) \qquad (92)
\end{aligned}$$

In analogy to Appendix B we expand the amplitudes into a power-series in the photon energy ω. With the definition

$$R = \frac{\Delta}{m_\pi} + \sqrt{\frac{\Delta^2}{m_\pi^2} - 1}$$

we find:

$$\begin{aligned}
Amp^{\Delta\pi}_{1+2} &= D\ \bar{u}(r)\ \Big\{\ -\epsilon\cdot\epsilon'\ \frac{2}{3}\ \Big[\ \frac{3}{2}\ \frac{d-2}{d-1}\ 2\ J_0(-\Delta, m_\pi^2) \\
&\qquad + \frac{\omega^2}{4\pi^2}\left(\frac{\Delta}{\Delta^2 - m_\pi^2} - \frac{m_\pi^2}{(\Delta^2-m_\pi^2)^{3/2}}\ \log R\right) + \mathcal{O}(\omega^4)\ \Big] \\
&\quad + [S_\mu\ ,\ S_\nu]\ \epsilon'^\mu \epsilon^\nu\ \frac{\omega}{6\pi^2}\ \Big[\ \frac{3}{d-1}\ 32\pi^2 L + 1 + 2\ \log(\frac{m_\pi}{\lambda}) \\
&\qquad + \frac{2\Delta}{\sqrt{\Delta^2 - m_\pi^2}} \log R + \omega^2\ \Big(\ \frac{\Delta m_\pi^2}{(\Delta^2-m_\pi^2)^{5/2}}\ \log R \\
&\qquad - \frac{\Delta^2 + 2m_\pi^2}{3\ (\Delta^2 - m_\pi^2)^2}\ \Big)\ + \mathcal{O}(\omega^4)\ \Big]\ \Big\}\ u(r)
\end{aligned} \tag{93}$$

$$\begin{aligned}
Amp^{\Delta\pi}_{3..6} &= D\ \bar{u}(r)\ \Big\{\ \epsilon\cdot\epsilon'\ \frac{1}{9\pi^2}\ \Big[\ \frac{9}{2}\ \frac{d-2}{(d-1)^2}\ 96\Delta L\pi^2 + 6\Delta \log(\frac{m_\pi}{\lambda}) \\
&\qquad - \Delta + 6\sqrt{\Delta^2 - m_\pi^2}\ \log R + \omega^2\ \Big(\ \frac{\Delta}{\Delta^2 - m_\pi^2} \\
&\qquad - \frac{m_\pi^2}{(\Delta^2-m_\pi^2)^{3/2}} \log R\ \Big)\ + \mathcal{O}(\omega^4)\ \Big] \\
&\quad + [S_\mu\ ,\ S_\nu]\ \epsilon'^\mu \epsilon^\nu\ \frac{\omega}{36\pi^2}\ \Big[\ 9\ \frac{-2}{(d-1)^2}\ 96\pi^2 L - 12\log(\frac{m_\pi}{\lambda}) - 10 \\
&\qquad - \frac{12\Delta}{\sqrt{\Delta^2 - m_\pi^2}}\ \log R + \omega^2\ \Big(\ \frac{\Delta^2 + 2m_\pi^2}{(\Delta^2-m_\pi^2)^2} \\
&\qquad - \frac{3\Delta m_\pi^2}{(\Delta^2-m_\pi^2)^{5/2}}\ \log R\ \Big)\ + \mathcal{O}(\omega^4)\ \Big] \\
&\quad - \epsilon\cdot k\ \epsilon'\cdot k\ \frac{1}{18\pi^2}\ \Big[\ \frac{1}{\sqrt{\Delta^2 - m_\pi^2}}\ \log R + \mathcal{O}(\omega^2)\ \Big] \\
&\quad + \ldots\ \Big\}\ u(r)
\end{aligned} \tag{94}$$

$$
\begin{aligned}
Amp^{\Delta\pi}_{7+8} &= D\ \bar{u}(r)\ \Big\{\ -\ \epsilon\cdot\epsilon'\ \frac{1}{72\pi^2}\ \Big[\ \frac{18(d-2)}{d\ (d-1)^2}\ 64(4d-1)\Delta L\pi^2 \qquad (95)\\
&\qquad +60\Delta\log(\frac{m_\pi}{\lambda})+60\sqrt{\Delta^2-m_\pi^2}\ \log R+\Delta\\
&\qquad +\omega^2\left(\frac{5\Delta}{\Delta^2-m_\pi^2}-\frac{5m_\pi^2}{(\Delta^2-m_\pi^2)^{3/2}}\ \log R\right)+\mathcal{O}(\omega^4)\ \Big]\\
&\quad -\ \epsilon\cdot\epsilon'\ \omega^2\ \frac{1}{36\pi^2}\ \Big[\ \frac{1}{\sqrt{\Delta^2-m_\pi^2}}\ \log R+\mathcal{O}(\omega^2)\ \Big]\\
&\quad +\ \epsilon\cdot k\ \epsilon'\cdot k\ \frac{1}{24\pi^2}\ \Big[\ \frac{1}{\sqrt{\Delta^2-m_\pi^2}}\ \log R+\mathcal{O}(\omega^2)\ \Big]\\
&\quad +\ ...\ \Big\}\ u(r)\\
Amp^{\Delta\pi}_{9} &= D\ \bar{u}(r)\ \epsilon\cdot\epsilon'\ \frac{1}{12\pi^2}\ \Big\{\ \frac{3}{2}\ \frac{d-2}{d-1}\ 96\Delta L\pi^2+6\Delta\log(\frac{m_\pi}{\lambda})-\Delta \qquad (96)\\
&\qquad +6\sqrt{\Delta^2-m_\pi^2}\ \log R\ \Big\}\ u(r)
\end{aligned}
$$

References

[1] J. Gasser and H. Leutwyler, Ann. Phys. (NY) **158**, 142 (1984) and Nucl. Phys. **B250**, 465 (1985).

[2] See, *e.g.* J.F. Donoghue, E. Golowich and B.R. Holstein, *Dynamics of the Standard Model*, Cambridge University Press, New York (1992).

[3] H. Bijnens, H. Sonoda and M.B. Wise, Nucl. Phys. **B261** (1985) 185.

[4] J. Gasser, M.E. Sainio and A. Svarc, Nucl. Phys. **B307**, 779 (1988).

[5] H. Georgi, Phys. Lett. **B240**, 447 (1990)

[6] E. Jenkins and A.V. Manohar, Phys. Lett. **B255**, 558 (1991).

[7] V. Bernard, N. Kaiser and U.-G. Meißner, Int. J. Mod. Phys. **E4**, 193 (1995).

[8] V. Bernard, N. Kaiser, J. Kambor and U.-G. Meißner, Nucl. Phys. **B388** (1992) 314.

[9] G. Ecker and M. Mojzis, Phys. Lett. **B365**, 312 (1996).

[10] E. Jenkins and A. Manohar, Phys. Lett. **B259**, 353 (1991); A. Falk, Nucl. Phys. **B378**, 79 (1992).

[11] M.N. Butler and M.J. Savage, Phys. Lett. **B294**, 369 (1992).

[12] T.R. Hemmert, B.R. Holstein and J. Kambor, "Systematic 1/M Expansion for Spin 3/2 Particles in Baryon Chiral Perturbation Theory," to be published in Phys. Lett. B.

[13] T.R. Hemmert, B.R. Holstein and J. Kambor, "Chiral Lagrangians and $\Delta(1232)$ Interactions," in preparation.

[14] F.J. Federspiel et al., Phys. Rev. Lett. **67**, 1511 (1991); E.L. Hallin et al., Phys. Rev. **C48**, 1497 (1993); A. Zeiger et al., Phys. Lett. **B278**, 34 (1992).

[15] J. Schmiedmayer et al., Phys. Rev. Lett. **66**, 1015 (1991).

[16] J.L. Friar, Ann. Phys. (NY), **95**, 170 (1975).

[17] V. Pascalutsa and O. Scholten, Nucl. Phys. **A591**, 658 (1995).

[18] B.R. Holstein, Comm. Nucl. Part. Phys. **20**, 301 (1992).

[19] A. L'vov, Phys. Lett. **B304**, 29 (1993).

[20] V. Bernard, N. Kaiser, A. Schmidt and U.-G. Meißner, Phys. Lett. **B319**, 269 (1993) and Z. Phys. **A348**, 317 (1994).

[21] N.C. Mukhopadhyay, A.M. Nathan and L. Zhang, Phys. Rev. **D47**, R7 (1993).

[22] M. Gell-Mann and M.L. Goldberger, Phys. Rev. **96**, 1433 (1954); F.E. Low, Phys. Rev. **96**, 1428 (1954).

[23] S.D. Drell and A.C. Hearn, Phys. Rev. Lett. **16**, 908 (1966); S. Gerasimov, Sov. J. Nucl. Phys. **2**, 430 (1966).

[24] A. Sandorfi, private communication.

[25] I. Karliner, Phys. Rev. **D7**, 2717 (1973).

[26] R.L. Workman and R.A. Arndt, Phys. Rev. **D45**, 1789 (1992).

[27] V. Burkert and Z. Li, Phys. Rev. **D47**, 46 (1993).

[28] L.N. Chang, Y. Liang and R.L. Workman, Phys. Lett. **B329**, 514 (1994).

[29] A.M. Sandorfi et al., Phys. Rev. **D50**, R6681 (1994).

[30] D. Drechsel, Prog. Part. Nucl. Phys. **34**, 181 (1995).

[31] T. Mannel, W. Roberts and Z. Ryzak, Nucl. Phys. **B368** (1992) 204.

[32] R.M. Davidson, N.C. Mukhopadhyay, and R.S. Wittman, Phys. Rev. **D43** (1991) 71.

[33] V. Bernard, N. Kaiser and U.-G. Meißner, Phys. Rev. Lett. **67**, 1515 (1991) and Nucl. Phys. **B373**, 364 (1992).

[34] S. Ragusa, Phys. Rev. **D47**, 3757 (1993) and Phys. Rev. **D49**, 3157 (1994).

[35] M. Benmerrouche, R.M. Davidson and N.C. Mukhopadhyay, Phys. Rev. **C39**, 2339 (1989).

FIGURE CAPTIONS:
Wiggly lines to the right (left) denote incoming (outgoing) photons, dotted lines denote pions and solid lines represent nucleons.

Figure 1: $O(\epsilon^2)$ Born graph in forward Compton scattering.

Figure 2: $O(\epsilon^3)$ Born contributions in forward Compton scattering.

Figure 3: $O(\epsilon^3)$ $N\pi$ Loop diagrams in forward Compton scattering.

Figure 4: $O(\epsilon^3)$ $\Delta\pi$ Loop diagrams in forward Compton scattering.

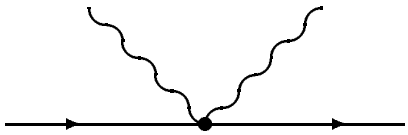

Figure 1: O(ϵ^2) Born graph in forward Compton Scattering.

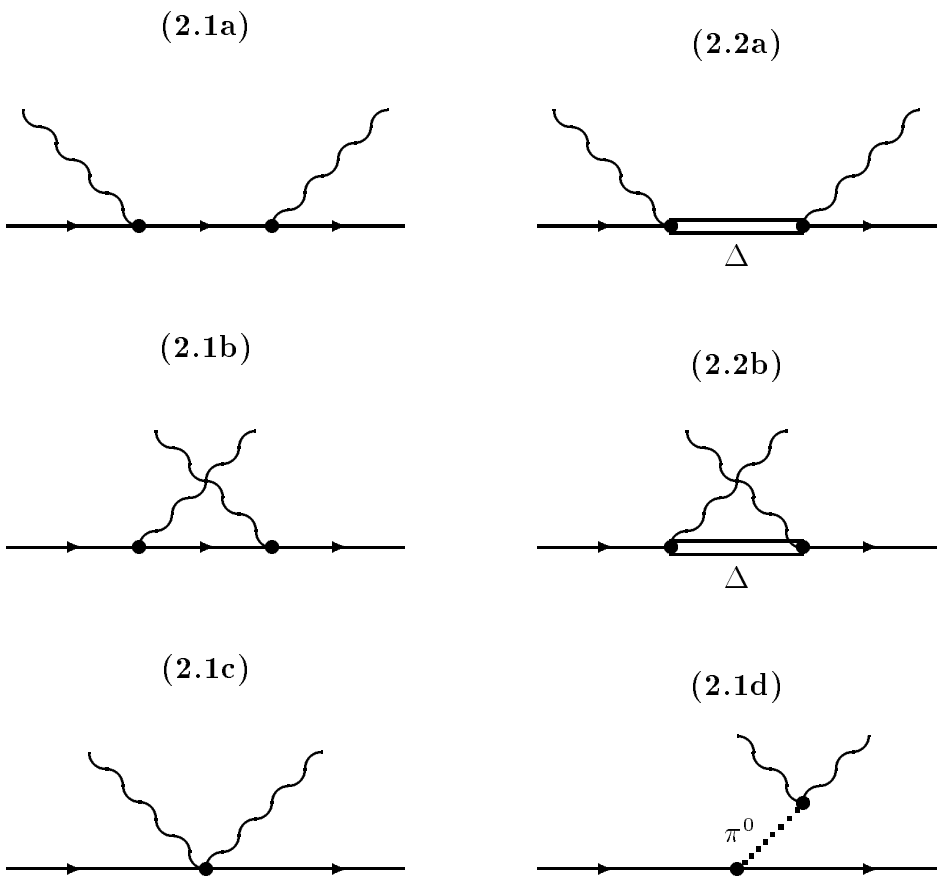

Figure 2: O(ϵ^3) Born graphs in forward Compton Scattering.

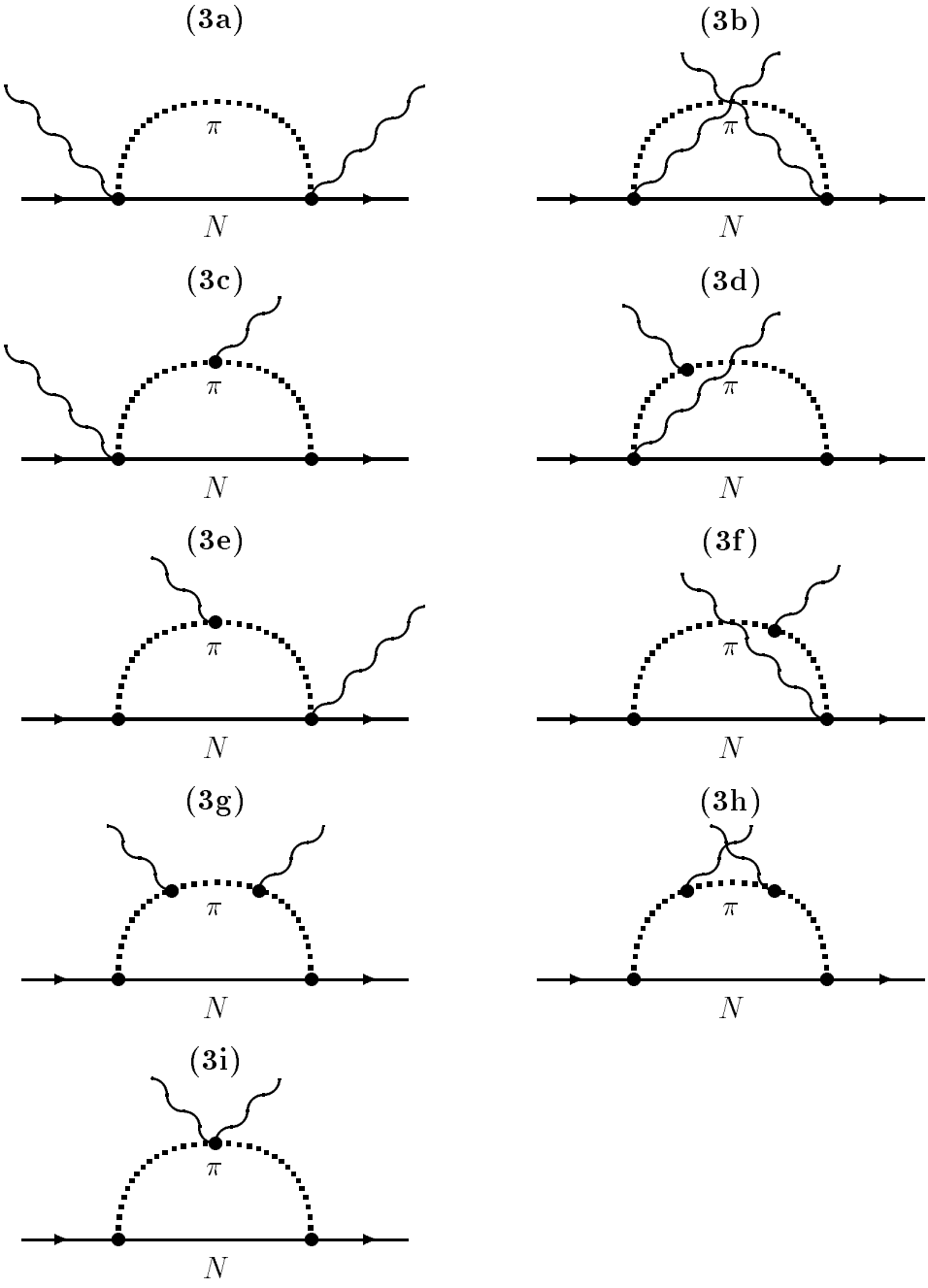

Figure 3: O(ϵ^3) $N\pi$ Loop Diagrams in Forward Compton Scattering.

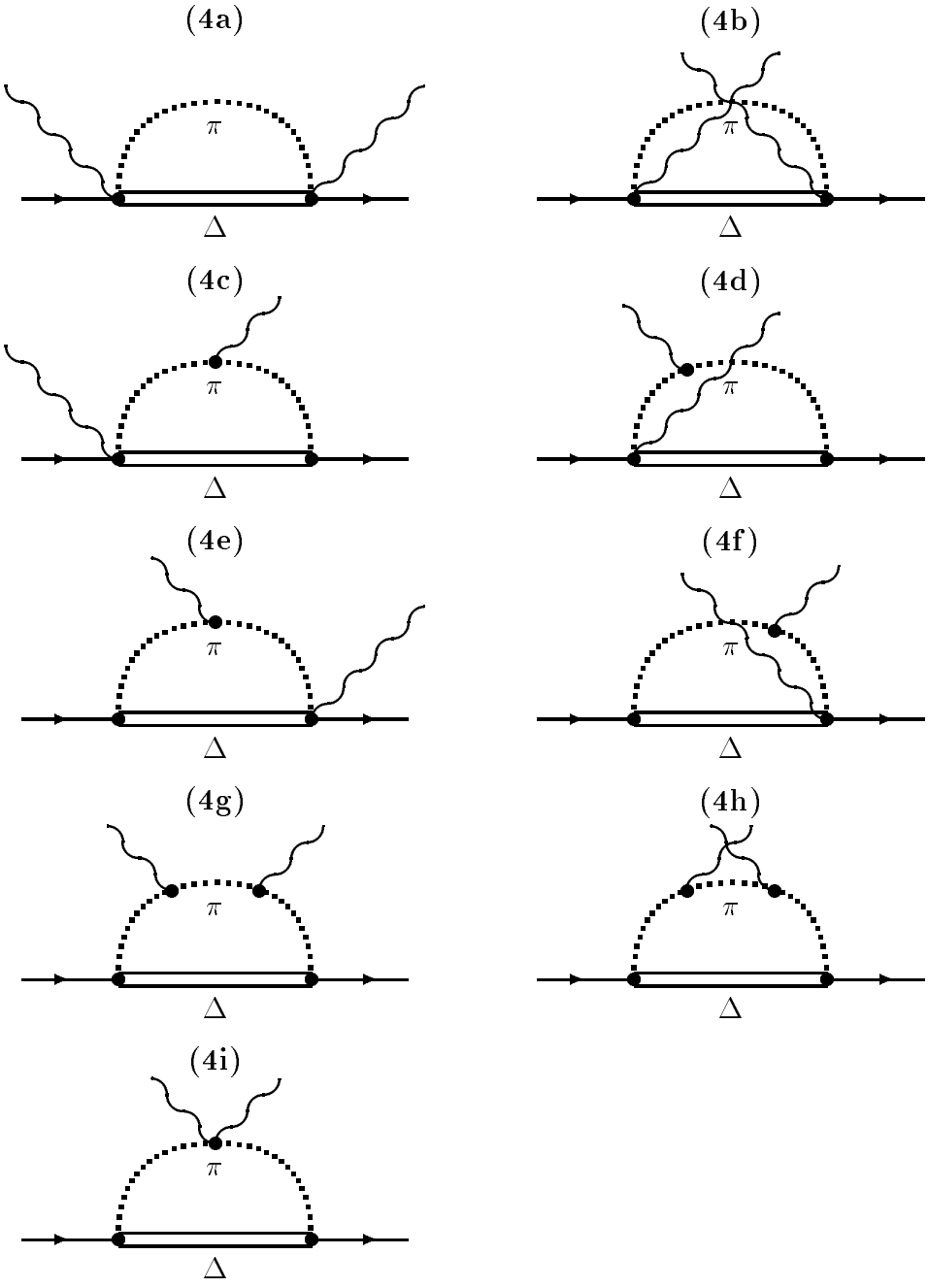

Figure 4: $O(\epsilon^3)$ $\Delta\pi$ Loop Diagrams in Forward Compton Scattering.